CHEMISTRY OF MATERIALS

Review

pubs.acs.org/cm

Chemistry of InP Nanocrystal Syntheses

Sudarsan Tamang,[†,§] Christophe Lincheneau,[∥,⊥,#] Yannick Hermans,[∥,⊥,#] Sohee Jeong,*[,†,‡] and Peter Reiss*[,∥,⊥,#]

[†]Nanomechanical Systems Research Division, Korea Institute of Machinery and Materials, Daejeon 305-343, Korea

[§]Department of Chemistry, Sikkim University, Gangtok 737102, India

[∥]Univ. Grenoble Alpes, INAC-SyMMES, F-38054 Grenoble Cedex 9, France

[⊥]CEA, INAC-SyMMES, Laboratoire d'Electronique Moleculaire, Organique et Hybride, 17 rue des Martyrs, F-38054 Grenoble Cedex 9, France

[#]CNRS, INAC-SPrAM (UMR 5819), F-38054 Grenoble Cedex 9, France

[‡]Department of Nanomechatronics, Korea University of Science and Technology (UST), Daejeon 305-350, Korea

ABSTRACT: Chemically synthesized InP nanocrystals (NCs) are drawing a large interest as a potentially less toxic alternative to CdSe-based nanocrystals. With a bulk band gap of 1.35 eV and an exciton Bohr radius of ~10 nm the emission wavelength of InP NCs can in principle be tuned throughout the whole visible and near-infrared range by changing their size. Furthermore, a few works reported fluorescence quantum yields exceeding 70% after overcoating the core NCs with appropriate shell materials. Therefore, InP NCs are very promising for use in lighting and display applications. On the other hand, a number of challenges remain to be addressed in order to progress from isolated research results to robust and reproducible synthesis methods for high quality InP NCs. First of all, the size distribution of the as-synthesized NCs needs to be reduced, which directly translates into more narrow emission line widths. Next, reliable protocols are required for achieving a given emission wavelength at high reaction yield and for further improving the emission efficiency and chemical and photostability. Advances in these directions have been hampered for a long time by the specific properties of InP, such as the rather covalent nature of binding implying harsh synthesis conditions, high sensitivity toward oxidation, and limited choice of phosphorus precursors. However, in recent years a much better understanding of the precursor conversion kinetics and reaction mechanisms has been achieved, giving this field new impulse. In this review we provide a comprehensive overview from initial synthetic approaches to the most recent developments. First, we highlight the fundamental differences in the syntheses of InP-based NCs with respect to established II–VI and IV–VI semiconductor NCs comparing their nucleation and growth stages. Next, we inspect in detail the influence of the nature of the phosphorus and indium precursors used and of reaction additives, such as zinc carboxylates or alkylamines, on the properties of the NCs. Finally, core/shell systems and doped InP NCs are discussed, and perspectives in this field are given.

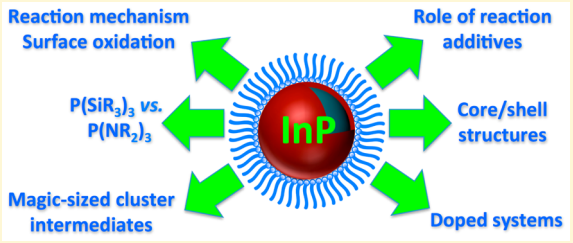

INTRODUCTION

By the end of last century semiconductor physics was a well-established field and so was the chemistry of colloids. However, following the seminal work of Efros, Ekimov, Brus, Henglein, and co-workers published in the early 1980s, the research on both colloidal particles and semiconductor materials took a new turn:[1−5] the size dependent optical properties in "very small" colloidal CdS particles had been established experimentally for the first time. It became clear that by controlling the size and shape of particles in colloidal form, electronic and optical properties of materials could be changed creating endless possibilities. This followed a renewed interest in the synthesis of semiconductor colloidal quantum dots (QDs). Initially there was skepticism on whether these semiconductor nanoparticles chemically synthesized in a flask could ever compete with or complement the materials produced by physical techniques in vacuum chambers. Nonetheless, over the last three decades synthetic schemes have been developed for high quality colloidal semiconductor nanocrystals (NCs),[6−14] which are now being investigated for use in various technologically and economically important fields such as photovoltaics, solid-state lighting, biological labeling and detection, etc. The recent market introduction of QD based displays is a testimony of this trend.[15] NCs synthesized via the colloidal route can provide advantages over epitaxially grown QDs such as (i) the size, shape, and composition of the particles can be controlled during synthesis; (ii) the surface of the particles can be modified via ligand exchange methods enabling the change of the solubility as well as of the functionality of the particles; (iii) the solvent processability facilitates cost-effective deposition techniques and device fabrication.

Received: January 4, 2016
Revised: March 29, 2016
Published: March 29, 2016

DOI: 10.1021/acs.chemmater.5b05044
Chem. Mater. 2016, 28, 2491−2506

Indium phosphide (InP) is one of the most widely studied semiconductor nanocrystals in colloidal form. It is a III−V semiconductor (bulk value of E_g: 1.35 eV) with a Bohr exciton radius of ∼10 nm.[16] In the strong quantum confinement regime its photoluminescence can be tuned from blue (∼480 nm) to the near-infrared (∼750 nm) by varying the size. Therefore, this material is of great interest especially for optoelectronics and biological imaging applications as a potential alternative to toxic cadmium and lead based colloidal NCs. In the EU for example, the use of Cd- and Pb-based materials in electrical and electronic equipment has been severely restricted by the RoHS (Restriction of Hazardous Substances Directive) directive. Comparably few studies on the toxicity of indium phosphide exist and there are no published reports specific to the toxicity of indium phosphide in humans. The International Agency for Research in Cancer (IARC) has concluded that there was sufficient evidence of carcinogenic activity of InP microparticles in mice and rats to classify indium phosphide in Group 2A (probably carcinogenic to humans).[17] This was based on long-term inhalation studies, in which the microparticles were administrated in the form of aerosols, leading to severe pulmonary inflammation and fibrotic changes. Such microparticles could occur for example during the processing (sawing, grinding, etc.) of indium phosphide ingots or wafers. However, no comparable data exists for colloidal InP NCs, which are around 1000 times smaller and show a completely different surface state with the presence of organic (ligands) and inorganic (shells) capping layers. Upon intravenous injection of InP/ZnS NCs in mice (25 mg/kg) no visible acute toxicity was observed after 12 weeks.[18] In addition to the direct impact of NCs exposure on target organs, the release of toxic ions is another possible mechanism driving toxicity of nanoparticles. Brunetti et al. compared the effect of Cd^{2+} and In^{3+} release from mercaptopropionic acid capped CdSe/ZnS and InP/ZnS nanocrystals.[19] CdSe/ZnS NCs were shown to induce cell mortality, oxidative stress, and increased intracellular Ca^{2+} content in two cell types, while InP/ZnS NCs did not. Chibli et al. showed that the cytotoxicity induced by the generation of reactive oxygen species (ROIs) was significantly lower in the case of InP/ZnS NCs as compared to CdTe/ZnS NCs.[20] Taken together, the available toxicity studies on InP based NCs indicate that these constitute a less toxic alternative to Cd-based quantum dots. At the same time the requirement of more systematic studies assessing the effects of InP NCs *in vitro* and *in vivo* is obvious.

Despite of the superiority of the more covalent III−V semiconductors as bulk electronic materials, in the form of NCs they have been outperformed so far by the more ionic II−VI and IV−VI compounds (e.g., CdSe, PbS). Covalent bond formation usually requires high temperatures, long reaction times, and reactive precursors.[21] As a consequence controlling the NC size becomes a major challenge in III−V semiconductors. For example, the narrowest fluorescence line widths (full widths at half maxima) obtained for InP NCs are on the order of 45−50 nm, whereas with Cd-based QDs emitting in the same wavelength range routinely values below 30 nm can be achieved. Recent optical studies on single particles have revealed that the emission line widths of CdSe and InP are nearly the same.[22] By consequence the broader line widths in ensembles of InP NCs compared to CdSe NCs are not due to an intrinsic material's property but result from their larger inhomogeneity in size. This effect could be accentuated if the dependence of the band gap on the NC size was more pronounced in the case of InP than for CdSe as expected due to the larger Bohr exciton radius (9.6 nm vs 4.6 nm).[23] Calculations using the effective mass model show this trend (Figure 1). On the other hand, more recent theoretical and experimental studies suggest that the effective mass model overestimates the size dependence of the excitonic band gap of InP.[24,25] Finally, InP is sensitive to oxidation, requiring stringent air-free conditions during synthesis and subsequent protection with an appropriate shell material. Today, fueled by the growing interest in improving the quality of InP based NCs substantial efforts are being made to achieve a better understanding of all stages of the synthesis reaction, including the underlying kinetics and reaction mechanisms.

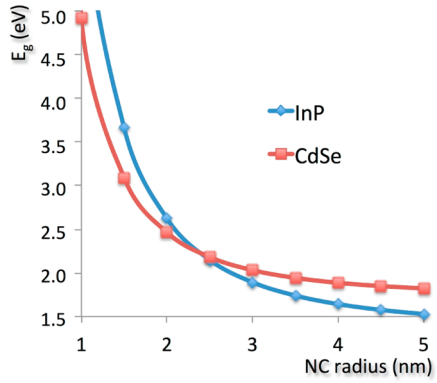

Figure 1. Dependence of the band gap on the nanocrystal diameter for InP and CdSe, calculated using the effective mass approximation (used parameters: E_g = 1.35/1.74 eV; ε_r = 12.4/9.5; r_{Bohr} = 9.6/4.6 nm for InP/CdSe).[23]

In contrast to more general reviews on semiconductor QDs, which also include III−V compounds,[26,27] here we focus on the underlying chemistry of the syntheses of colloidal InP NCs and on the current understanding of factors that affect their size, size distribution, crystallinity, fluorescence quantum yield, and stability with special emphasis on the most recent developments. InP NC may also serve as a basis and prototype for the synthetic development of other III−V semiconductor materials including InAs, GaAs, GaP, InSb, etc. with similar bonding nature and precursor chemistry.

1. EVOLUTION OF THE SYNTHESIS METHODS FOR InP NANOCRYSTALS

Wells' dehalosilylation reaction has been initially the most commonly followed route to synthesize InP NCs.[28−30] In this approach indium(III) halide is reacted with tris(trimethylsilyl)-phosphine ($P(SiMe_3)_3$). Healy, Wells, and co-workers[28,29] showed that the formation of InP NCs proceeds via the formation of adduct complexes between the indium and phosphorus precursors, followed by the stepwise elimination of Me_3SiCl (Scheme 1). In this reaction the elimination of trimethylsilylhalide is the rate-limiting step.[29] At room temperature, the 1:1 molar reaction between InI_3 and $P(SiMe_3)_3$ yields the yellow 1:1 adduct $I_3In{-}P(SiMe_3)_3$. Upon heating to 150−225 °C a weight loss of 58.6% per mole was observed corresponding to 2 mol of Me_3SiI followed by an additional loss of 26.3% at 240−280 °C. The residue remaining was 19.5% of the original weight of the adduct, corresponding to InP. In the chlorine variant of this reaction,[28] when adding $P(SiMe_3)_3$ (5% excess) to a toluene suspension of

DOI: 10.1021/acs.chemmater.5b05044
Chem. Mater. 2016, 28, 2491−2506

Scheme 1. Proposed Mechanism of Wells' Dehalosilylation Reaction between Indium(III) Chloride and Tris(trimethylsilyl)phosphine[a]

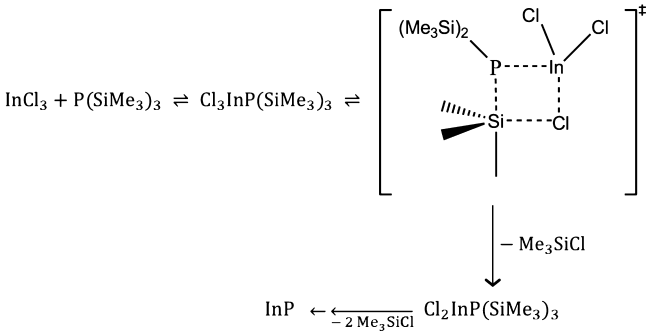

[a]It has been suggested that the intermediate II exists in oligomer form, $[Cl_2InP(SiMe_3)_2]_x$. Reproduced with permission from ref 29. Copyright 1995 American Chemical Society.

$InCl_3$ at −78 °C a pale yellow solid was formed, which deepened color as the reaction temperature was raised to room temperature.

The product was isolated, and based on X-ray photoelectron spectroscopy (XPS) and elemental analysis the orange powder has been identified as the oligomer $[Cl_2InP(SiMe_3)_2]_x$. Elimination of Me_3SiCl was observed from this intermediate when heated to 150 °C. However, using X-ray diffraction the formation of crystalline InP particles could only be detected when the last equivalent of Me_3SiCl was eliminated by heating at 650 °C for 1 h under vacuum. Mićić et al. synthesized for the first time colloidal InP QDs using a modification of the original dehalosilylation reaction where chloroindium oxalate was heated with $P(SiMe_3)_3$ in trioctylphosphine oxide (TOPO) at 270 °C for 3 days.[31] The same approach has been extended to the synthesis of GaP, $InGaP_2$ and GaAs QDs.[32] Heath and co-workers improved the size distribution of InP NCs obtained by the same method using size-selective precipitation, which allowed putting into evidence their size-dependent optical properties.[33] Furthermore, the oxidation of In and P surface sites has been demonstrated by XPS studies. TOPO had been introduced in the synthesis of CdE (E = S, Se, Te) NCs in the pioneering work of Murray, Norris, and Bawendi.[6] This compound plays the double role of reaction medium/solvent and surface ligand and is therefore classified as coordinating solvent. Due to its high boiling point, TOPO allows reactions to be carried out at temperatures as high as 350 °C. In the case of InP, however, the slow progression of the reaction led to very long reaction times. This together with the large size distribution of the as-synthesized NCs motivated further research. A milestone in the quest for high quality InP NCs has been achieved by Peng et al., who first proposed 1-octadecene as a noncoordinating solvent in combination with fatty acid type stabilizing ligands.[11] Again, a similar approach had prior been used for the synthesis of monodisperse CdS and other II−VI semiconductor NCs.[34] Today, nearly all $P(SiMe_3)_3$ based InP NCs syntheses involve its reaction with an indium(III) precursor at elevated temperature (180−300 °C) in 1-octadecene and invariably in the presence of stabilizing ligands such as fatty acids,[11,13] amines[9] and/or alkylphosphines[31,33] (cf. Table 1). The details of these syntheses as well as more recent developments will be discussed in the subsequent sections.

Table 1. Commonly Used Chemicals in the Synthesis of InP Nanocrystals

chemical	name	role
$C_{16}H_{33}C{=}CH_2$	1-octadecene (ODE)	solvent (noncoordinating)
$C_8H_{17}C{=}CC_8H_{16}NH_2$	oleylamine	solvent/ligand
$(C_8H_{17})_3P$	trioctyl phosphine (TOP)	solvent/ligand
$(C_8H_{17})_3P{=}O$	trioctyl phosphine (TOPO)	solvent/ligand
$C_8H_{17}NH_2$	octylamine	"Activator" (cf. Section 33)
$CH_3(CH_2)_nCOOH$ n = 10, 12, 14, 16	fatty acid	ligand, complexing agent
$[(CH_3)_3Si]_3P$	tris(trimethylsilyl) phosphine (PTMS)	P precursor
PH_3	phosphine	P precursor
InX_3, X = carboxylate, halide	indium salt	In precursor
ZnX_2, X = carboxylate, halide	zinc salt	Zn precursor, ligand

2. NUCLEATION AND GROWTH

The formation of nanocrystals from homogeneous solution is governed by the two distinct stages of nucleation and growth. Understanding the kinetics of these processes and the underlying chemical reactions is primordial for the rational design of synthesis methods. Experimentally such studies are challenging due to the short time scale, small dimensions, and stringent experimental conditions (e.g., elevated temperature, inert atmosphere) generally involved. Studies of the past decade have demonstrated that nucleation is preceded by the transformation of molecular precursors or macromolecular precursor complexes into the smallest notional building blocks of the crystal, termed as monomers.[35,36] By consequence NC synthesis can be described as a two-step reaction:[37]

$$\text{Precursors} \rightarrow \text{Monomers} \rightleftharpoons \text{Nanocrystals}$$

When the monomer concentration exceeds the critical threshold value of the given reaction, nucleation takes place via condensation of the monomers from solution. To be thermodynamically stable the formed nuclei need to attain a minimum critical radius given by eq 1:

$$r_c = \frac{2\gamma V_m}{RT \ln S} \quad (1)$$

where γ is the surface free energy per unit area, V_m is the molar volume of the particle, R is the universal gas constant, T is the absolute temperature, and S is the supersaturation.[38] Below the critical radius ($r < r_c$) the nuclei dissolve, largely due to their high surface free energy, while for $r > r_c$ they grow in size. In the growth stage further size increase takes place from the remaining monomer reservoir. The precise control of the growth stage is complicated by the fact that monomers can also be supplied by dissolution of already formed NCs. The smallest particles with the highest surface free energy are most prone to this process, which leads to a decrease of NC number and increase of mean size. This process is called Ostwald ripening or Lifshitz−Slyozov−Wagner growth and leads to a linear increase of the cube of the average diameter with time, resulting in an increase of polydispersity.[39] As will be shown in Section 3, this process is the predominant growth mechanism for InP NCs synthesized using $P(SiMe_3)_3$ as the phosphorus precursor. In the following we will discuss the different factors controlling

DOI: 10.1021/acs.chemmater.5b05044
Chem. Mater. 2016, 28, 2491−2506

size and size distribution in NC syntheses using hot-injection and heat-up approaches.

Separation of Nucleation and Growth. The seminal work of LaMer and Dinegar[40] led to the model depicted in Figure 2, which describes the different stages of the formation

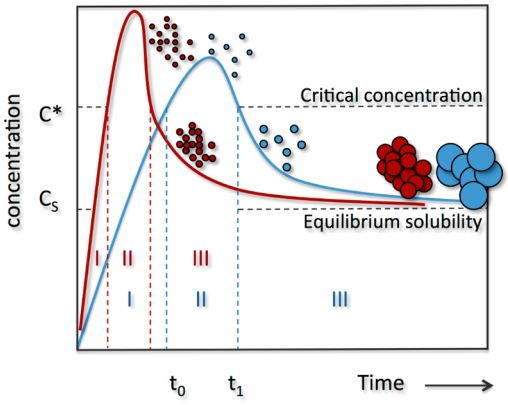

Figure 2. LaMer plot for the synthesis monodisperse particles describing the formation of monodisperse NCs following three well separated stages:[40] (I) Precursor conversion and increase of the monomer concentration above the critical concentration C*; (II) nucleation; and (III) growth of the NCs from solution while the monomer concentration is in the regime of supersaturation ($C_s < C < C^*$). A high precursor-to-monomer conversion rate (red curve) leads to a larger number of NCs of smaller final size than in the case of a low conversion rate (blue curve).

of colloids from homogeneous solution. Importantly, the temporal separation of nucleation and growth has been shown to be essential for obtaining monodisperse colloidal NCs.

In this scheme, a rapid burst of nucleation followed by a slow growth stage is desired. Usually the "hot-injection" method is employed to achieve this separation.[41,42] In this method, the precursor(s) solution at room temperature is rapidly injected into the hot reaction medium, which triggers monomer formation and the burst of nucleation. Within seconds, the solution temperature drops, with the concomitant drop of monomer concentration due to nuclei formation terminating the nucleation process. Subsequently, the growth stage takes over with no further nuclei being formed. The hot-injection method is the most widely used technique for synthesizing colloidal InP NCs. The "heat-up" method is an alternative approach, in which the reaction mixture containing precursors, stabilizing ligands, and solvent(s) is heated from room temperature to elevated temperatures.[41,43,44] In the first stage of this reaction monomer generation and accumulation takes place upon heating, leading to the increase of supersaturation until the critical value for nucleation is reached. In contrast to the hot-injection approach, the nucleation period in heat-up syntheses can be much longer, on the same order as the growth period. The choice of precursors and heating rate is of paramount importance for obtaining high quality NCs in this reaction scheme. A comprehensive review by van Embden et al. focusing on this technique discusses how the choice of precursors, ligands, and reaction conditions affects the nucleation and growth stages.[44] In comparison with the hot-injection method, the heat-up method can simplify the scale-up of syntheses and improve reproducibility. The solvothermal synthesis can be considered as a variant of this approach. It takes place under increased pressure in a closed reaction vessel (autoclave), and some examples of the solvothermal synthesis of InP NCs exist.[45−47]

Influence of the Precursor Conversion Rate. Adapting the precursor conversion rate can be an effective means for tuning the size while maximizing reaction yield and minimizing size distribution.[48] This is possible because many NC synthesis reactions reach a point at full yield where the diameter remains quasi-constant and the size dispersion is close to its minimum value. The size reached at this "end point" of the reaction directly depends on the number of nuclei initially formed. A straightforward way for influencing this number is by tuning the rate constant of monomer formation. At constant total amount of precursors, higher precursor-to-monomer conversion rates lead to smaller final NC diameters due to the larger number of nuclei formed (cf. Figure 2). Kinetic models have been proposed by the groups of Hens, Owen, and Bawendi with the goal to describe quantitatively the correlation between precursor conversion rate and size/size distribution.[37,49,50] A high tunability has been achieved by varying this parameter with NCs of II−VI and IV−VI compounds.[36,49,51] However, recent studies indicate that the variation of the precursor conversion rate leads to much lower tunability in the case of III−V semiconductors.[52] In particular the use of less reactive precursors like tris(trimethylgermyl) phosphine instead of tris(trimethylsilyl)phosphine did not allow switching from a ripening type growth to homogeneous growth from solution, and therefore the size distribution remained comparably broad.[53] The use of tris(triphenylsilyl)phosphine, in turn, slowed down the precursor conversion too much, leading to the inability of separating nucleation and growth and resulting in a broad size dispersion.[54] An important feature of synthetic schemes giving access to monodisperse II−VI and IV−VI NCs is the possibility of reaching a regime of "size-focusing" during the growth stage. As will be shown below, conducting particle growth under high monomer concentration allows over-compensating detrimental effects arising from uncontrolled Ostwald ripening and narrowing down an initially broader size distribution. This behavior is not predicted by the LaMer model. Initial theoretical works of Reiss[55] and subsequent studies by Sugimoto[38] confirmed size focusing to occur in the case of diffusion controlled NC growth.

Diffusion and Reaction Controlled Growth. NC growth requires the diffusion of monomers toward the surface of the growing crystal and the reaction of the monomers on the surface. If the diffusion coefficient D of the monomer is smaller than rate constant k for the surface reaction (reaction controlled growth), the rate of size increase becomes independent of the particle size, i.e.,

$$\frac{dr}{dt} = kV_m(C_b - C_e) \tag{2}$$

where V_m is the crystal molar volume, C_b the concentration of monomers in the bulk of the solution, and C_e the solubility of the particle, which is a function of its size.[38] This size-dependent solubility of the particle is given by the Gibbs−Thomson equation

$$C_e = C_\infty e^{(2\sigma V_m/rRT)} \tag{3}$$

where C_∞ is the solubility of a particle of infinite dimension, σ the specific surface energy, R the universal gas constant, and T the absolute temperature. Reaction controlled growth leads to

DOI: 10.1021/acs.chemmater.5b05044
Chem. Mater. 2016, 28, 2491−2506

broader size distributions than diffusion controlled growth due to the size independent growth rate (cf. eq 2).[38,56] In the case of diffusion controlled growth ($D \ll k$), the rate of size increase is given by

$$\frac{dr}{dt} = \frac{DV_m}{r}(C_b - C_e) \tag{4}$$

If the difference between the solubility of the crystal C_e and the monomer concentration C_b is constant,

$$\frac{dr}{dt} \propto \frac{1}{r} \tag{5}$$

i.e., smaller particles will grow at faster rates than larger ones, and the size distribution decreases with time.[38] Experimentally, however, $(C_b - C_e)$ is not a constant but strongly influenced by fluctuations of the monomer concentration.

Influence of the Monomer Concentration during the Growth Stage. A drop in the monomer concentration pushes the system toward equilibrium solubility. Consequently, Ostwald ripening begins and defocusing of the size distribution takes place.[57] It is therefore necessary to maintain a high monomer concentration during diffusion controlled growth in order to drive the reaction toward the size focusing regime.[38] By combining eqs 3 and 4, the growth rate of a single particle of radius r is

$$\frac{dr}{dt} = \frac{k_D}{r}\left(\frac{1}{r^*} - \frac{1}{r}\right) \tag{6}$$

where $k_D = 2\sigma DV_mC_\infty/RT$ and r^* is the equilibrium size for a given concentration showing zero growth rate (Figure 3). The

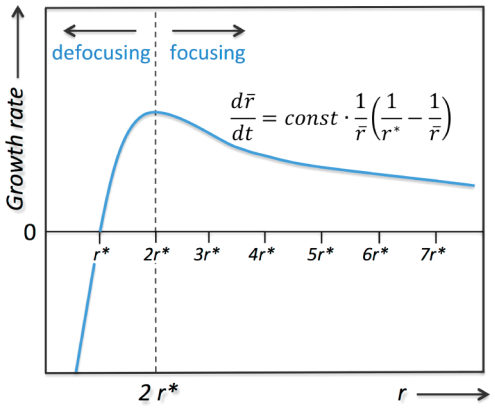

Figure 3. (a) Size-dependent growth rate in the diffusion controlled growth of NCs. For the average radius $\bar{r} > 2r^*$ size focusing occurs, while for $\bar{r} < 2r^*$ the size distribution broadens. Adapted with permission from ref 38. Copyright 1987 Elsevier. r^* indicates for a given concentration the equilibrium size of zero growth rate.

maximum growth rate occurs at $r = 2r^*$, and size focusing takes place for $r > 2r^*$. As r^* decreases under depletion of the monomer reservoir, it can be practically necessary to supply additional monomers during the growth stage. This can be experimentally achieved by means of multiple precursor injections as demonstrated by Peng and co-workers in the synthesis of CdSe and InAs NCs.[58]

In addition to multiple injections, the use of more stable precursors is another strategy to maintain a high monomer concentration during the growth stage. For example, by replacing $As(SiMe_3)_3$ with more stable $As(GeMe_3)_3$ the size distribution of InAs NCs could be improved.[53] Clark et al. showed that by increasing the rate of monomer production during the growth stage Ostwald ripening can be stopped[59] and eq 6 can be reduced to

$$\frac{dr}{dt} \propto \frac{k_D}{r} \tag{7}$$

Consequently, smaller NCs catch up with the larger ones resulting in reduced polydispersity, while the extent of focusing depends on both the monomer production rate and the number of NCs. The seeded growth technique where nuclei are supplied in the reaction mixture from an external source has been suggested as a strategy for controlling these two parameters independently.[59]

3. PHOSPHORUS PRECURSORS

The comparably broad size distribution of as-synthesized InP NCs with respect to II−VI and IV−VI systems indicates that separation of nucleation and growth is more difficult to achieve. Two causes have often been cited for this: first, the more covalent nature of the III−V precursors;[21] second, the fast depletion of molecular precursors at high temperature.[60] The first factor makes it comparably difficult to find precursors, which can be transformed to monomers of appropriate reactivity. Indium complexes of high stability require high reaction temperatures and long reaction times to initiate nucleation and growth. Under these conditions it can become impossible to enforce LaMer type growth.[21] Second, Allen et al. found that the $P(SiMe_3)_3$ precursor depletes very quickly at high reaction temperature leaving no molecular phosphorus precursor available for monomer production during the growth stage.[60] In this situation growth proceeds via Ostwald ripening, which is associated with increased polydispersity (cf. Section 2).[59] The rapid depletion of the phosphorus precursor in the hot reaction solution surely contributes also to the difficulty of synthesizing NIR (>700 nm) emitting InP NCs. The growth of larger sized InP NCs using $P(SiMe_3)_3$ has only been possible by means of multiple injections of the precursor solutions.[9]

Prior to the study of Allen and Bawendi[60] several possible replacements for $P(SiMe_3)_3$ were already investigated with the goal to find suitable precursors of lower cost and toxicity. As such white phosphorus (P4),[61] $In(tBu_2P)_3$,[62] Na_3P,[63] PCl_3,[64] and gaseous phosphine (PH_3)[65] were explored leading to mitigated results. P_4 was used in a solvothermal approach that yielded polydisperse and aggregated InP NCs. The same phosphorus source was applied in a low temperature (70 °C) synthesis using indium chloride and sodium borohydride in an ethanol/toluene mixture. In this case the *in situ* reaction of In^0 with P^0 is supposed to take place after reduction of $InCl_3$ with $NaBH_4$. However, once again rather polydisperse (3−6 nm) and aggregated InP NCs were obtained, even though X-ray diffraction and Raman spectroscopy confirmed their high crystallinity.[61] InP NCs of improved optical properties were obtained with $In(tBu_2P)_3$[62] and Na_3P,[63] but in both cases there were difficulties to control particle size and, thus, the band gap. Size tunability could be obtained when PCl_3 and indium acetate ($In(OAc)_3$) were used in a low temperature coreduction approach with $LiBHEt_3$ as reducing agent.[64] However, still the size distribution was broader for InP NCs made with PCl_3 than with $P(SiMe_3)_3$. A less expensive alternative to $P(SiMe_3)_3$ was proposed in form of *in situ* produced phosphine gas PH_3 from M_3P_2 (M = Ca or Zn) and acid (e.g., H_2SO_4, HCl).[65] By

DOI: 10.1021/acs.chemmater.5b05044
Chem. Mater. 2016, 28, 2491−2506

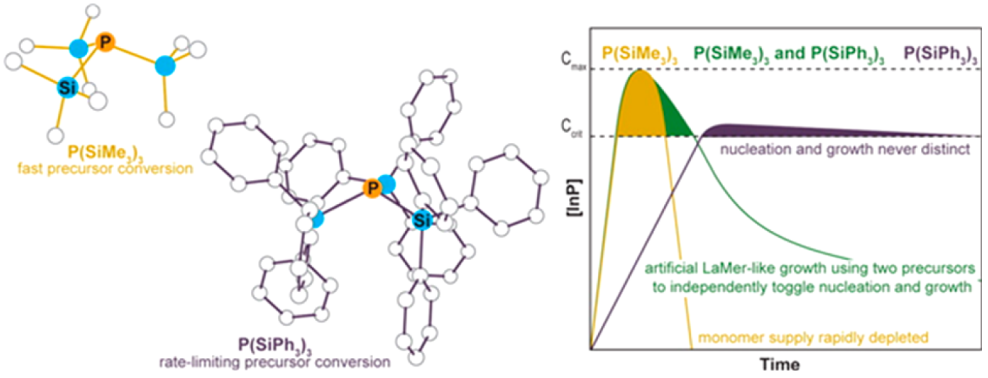

Figure 4. LaMer-like growth in the synthesis of InP NCs by using two phosphorus precursors of different reactivity. Reproduced with permission from ref 54. Copyright 2014 American Chemical Society.

bubbling PH_3 through a mixture of $In(OAc)_3$ and myristic acid in ODE, InP NCs with an emission ranging between 570 and 720 nm were obtained.

To circumvent the problem of rapid precursor depletion in $P(SiMe_3)_3$ based methods, more recently phosphorus precursors of higher stability have been synthesized. For example, by substitution of one of the methyl groups bound to silicon with a sterically demanding tertiary butyl group resulting in $P(SiMe_2(t\text{-}Bu))_3$, access to larger-sized InP QDs was possible without sacrificing a narrow size distribution, shifting the emission wavelength from 600 to 640 nm.[66] Gary et al. attempted enforcing LaMer-like growth by tuning the reactivity of the phosphorus precursor by adding a compound of lower reactivity ($P(SiPh_3)_3$) to $P(SiMe_3)_3$.[54] The latter led to rapid nucleation while the former was supposed to ensure the supply of molecular precursors during the growth stage (Figure 4).

However, the particle size was limited to a range of 2.3−3.7 nm, and the size distribution was still poor as compared to high quality II−VI or IV−VI NCs. The authors conclude that separation of nucleation and growth is not a sufficient criterion to obtain monodisperse NCs in the covalent InP system. Harris et al. introduced another more stable phosphorus precursor, $P(GeMe_3)_3$, replacing the Si−P bonds by Ge−P bonds.[53,67] Reaction kinetics of the InP NC synthesis using this phosphorus precursor were studied using *in situ* UV−vis spectroscopy and NMR analysis. Although the precursor conversion was found to be more than four times slower compared to $P(SiMe_3)_3$, its completion still preceded particle growth leading to no significant improvement in the size distribution. More recently, Cossairt and co-workers reported on a two-step nucleation and growth model for InP NCs through so-called magic sized cluster (MSC) intermediates (Figure 5).[68] In this context, MSCs can be defined as inorganic clusters of a specific size with a significantly higher thermodynamic stability relative to clusters of other sizes.

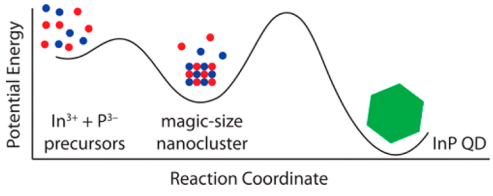

Figure 5. Growth mechanism of InP NCs implying magic-sized clusters as reaction intermediate. Reproduced with permission from ref 68. Copyright 2015 American Chemical Society.

MSCs have been observed in the syntheses of various other types of semiconductor NCs including CdSe,[69−71] CdS,[72] CdTe,[69] PbSe,[73] and InAs.[74,75] For temperatures up to 120 °C the reaction of indium myristate with $P(SiMe_3)_3$ led to the formation of kinetically persistent MSCs as observed by a recurring distinct peak at 368 nm in UV−vis spectra.[68] Subsequently, heterogeneous growth of InP NCs was observed forming NCs with an initial diameter of approximately 3 nm. This behavior was explained by a second nucleation process where InP nuclei precipitated out of a supersaturated monomer solution, created by the destabilization of the MSCs. A direct consequence of this second nucleation mechanism is that maintaining a steady monomer reservoir, through fine-tuning of the phosphorus precursor reactivity, is impossible when monomers are supplied via MSCs decomposition. However, as indicated in this work the obtained MSCs could serve as a single source precursor for InP NC synthesis; injection of the MSCs into hot squalane (400 °C) led to InP NCs of 3.1 ± 0.5 nm size.[68] Gary and co-workers also reported the first single crystal X-ray structure of 1.3 nm InP magic-sized nanoclusters passivated by phenylacetate ligands.[76] The isolated cluster $In_{37}P_{20}(O_2CR)_{51}$ (R = CH_2Ph) possesses a nonstoichiometric core composed of fused 6-membered rings, with atom arrangements strongly deviating from zinc blende or wurtzite structures. Thus, in addition to their potential role as single source precursors, MSCs are an important class of reaction intermediates that can offer unique insights into the formation mechanisms of InP NCs as well as their crystal structure and surface state/ligand binding modes.

Yang and co-workers reported a novel synthesis method using the cheaper and easier to handle aminophosphine precursor tris(dimethylamino)phosphine, $P(NMe_2)_3$, instead of $P(SiMe_3)_3$.[77] In this procedure, oleylamine is applied as coordinating solvent/ligand in combination with indium chloride and zinc chloride. Earlier reports where $P(NMe_2)_3$ was successfully used in solvothermal methods paved the way for its application in such a hot injection approach.[78] It should be noted that reactions using indium carboxylate as In precursor or ODE as the solvent failed with this phosphorus precursor. The obtained InP NCs present a tunable excitonic absorption peak from 530 nm (green) to 610 nm (red), albeit no PL signal. After growth of a ZnS shell fluorescence emission with a line width of ∼60 nm and a QY of ∼50% was obtained. Tessier et al. expanded this approach using $P(NEt_2)_3$ and demonstrating that size tuning at full reaction yield is possible by changing the nature of the indium halide used as the In precursor:[79] the lighter the halide (I, Br, Cl), the smaller the

DOI: 10.1021/acs.chemmater.5b05044
Chem. Mater. 2016, 28, 2491−2506

band gap and hence larger the NC size. The emission line width obtained after overgrowth with a ZnS or ZnSe shell is 46−64 nm (fwhm) comparable to the best values obtained for as-synthesized InP NCs using $P(SiMe_3)_3$, and the range of emission is 510−630 nm. As in Yang's method[77] also $ZnCl_2$ was used during InP core synthesis. Control experiments without Zn addition resulted in an enlarged size distribution as seen from the broader absorption features (Figure 6).

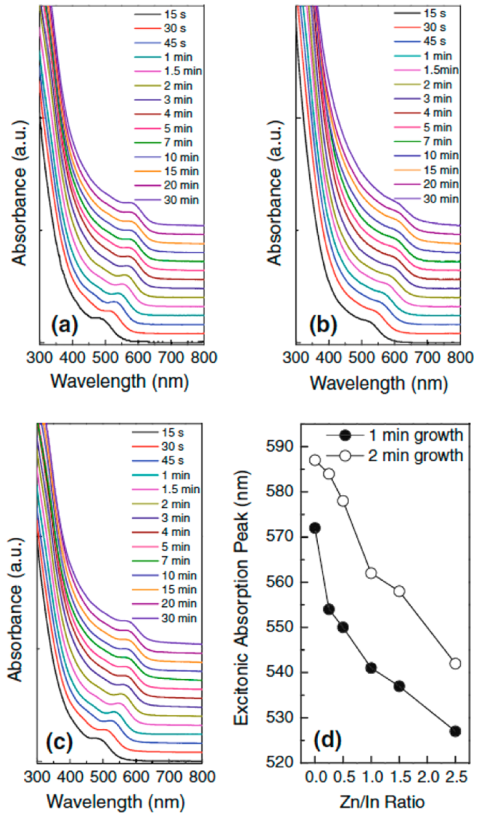

Figure 6. Temporal evolution of the absorption spectra of InP NCs synthesized using $P(NMe_2)_3$ as the phosphorus precursor and Zn:In ratios of 1 (a), 0 (b), and 1.5 (c). (d) Excitonic peak wavelength after 1 and 2 min of growth using Zn:In ratios between 0 and 2.5. Reproduced with permission from ref 77. Copyright 2013 Springer Science+Business Media Dordrecht.

Furthermore, increasing the Zn:In ratio led to an increase of the band gap. However, even a large amount of Zn introduced in the beginning of the reaction (1:1) resulted in a final In:Zn ratio of 13−14. Therefore, the authors concluded that Zn atoms were surface bound. Very recently the synthesis of high quality tetrahedron shaped InP quantum dots has been achieved by reacting $InCl_3$ and $P(NMe_2)_3$ in oleylamine without the use of $ZnCl_2$.[80]

4. INDIUM PRECURSORS, LIGANDS, AND REACTION ADDITIVES

The large majority of syntheses uses simple In(III) salts such as indium halides or indium acetate as the indium precursor. These are transformed during the first step of the reaction into reactive species, soluble in the used solvent. This step, generally taking place at an intermediate temperature of approximately 100 °C, involves the reaction of the indium salt with an appropriate complexing agent, such as a high boiling point carboxylic acid (fatty acid). Sporadic examples of the use of organometallic indium precursors like trimethylindium ($InMe_3$) can also be found. Xu et al. reacted for instance $InMe_3$ with $P(SiMe_3)_3$ in weakly coordinating fatty acid esters (e.g., methyl myristate) and in the presence of protic agents (e.g., dioctylamine, hexadecylamine).[9] This approach yielded small-sized InP QDs of comparably narrow size distribution and emission line width (48 nm, fwhm). It was hypothesized that the addition of protic agents led to the hydrolyzation of $P(SiMe_3)_3$ resulting in accelerated reaction kinetics.

The fatty acids used as complexing agents act in most cases also as surface ligands of the obtained InP NCs. The addition of primary amines and of zinc carboxylates can result in improved optical properties, in terms of the spectral range of emission and fluorescence quantum yield, as discussed in the following sections.

4.1. Role of Fatty Acids Used as Complexing Agent/Surface Ligands. Initially the reaction time of the synthesis of InP NCs in the coordinating solvent TOPO was 3−7 days, i.e., much longer than for their II−VI counterparts.[31] This was dramatically decreased to durations of minutes to hours by carrying out the reaction in the noncoordinating solvent 1-octadecene (ODE), in the presence of fatty acids.[11] Fatty acids enable the solubilization of the indium precursor in ODE and act as surface ligands for the formed InP NCs due to the presence of the coordinating carboxylic acid functional group. In a typical reaction $P(SiMe_3)_3$ diluted in ODE is injected into a solution of the complexed In precursor in ODE, which has been heated to elevated temperature (250−300 °C).

As shown in Figure 7, the size distribution of the NCs was found to be dependent on the length of fatty acid alkyl chain.[11]

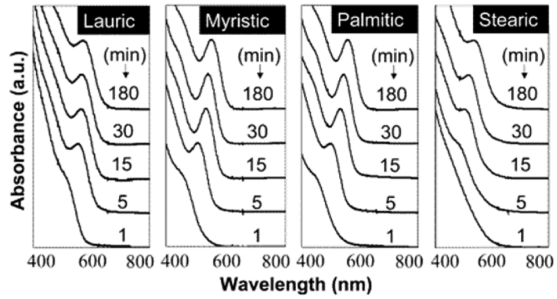

Figure 7. Evolution of the UV−vis absorption spectra of InP nanocrystals grown with fatty acids of different alkyl chain length as the surface ligands. In:fatty acid ratio = 1:3 for all reactions. Reproduced with permission from ref 11. Copyright 2002 American Chemical Society.

For example, myristic acid (C_{14}) and palmitic acid (C_{16}) yielded the best results as evident from the sharp absorption peaks in the UV−vis spectra. The authors suggested that these fatty acids provided balanced nucleation and growth rates. The In:P:fatty acid ratio was optimized to 1:0.5:3. Many InP QD syntheses in noncoordinating solvent involve variations of this reaction scheme. In the absence of any competing pathways, the same mechanism for the formation of InP NCs is supposed to take place as in the dehalosilylation reaction discussed above (Scheme 1). However, subsequent studies by Nayral, Delpech, and co-workers indicate that side reactions play an important role in this synthesis.[81,82] They carried out a coupled XPS, FTIR, and NMR study on the surface chemistry of InP NCs, synthesized using palmitic acid as the complexing agent/surface ligand. This study revealed that at elevated temperature the

DOI: 10.1021/acs.chemmater.5b05044
Chem. Mater. 2016, 28, 2491−2506

carboxylic acid is prone to a side reaction yielding a dialkylketone (palmitone) under release of water (Figure 8).

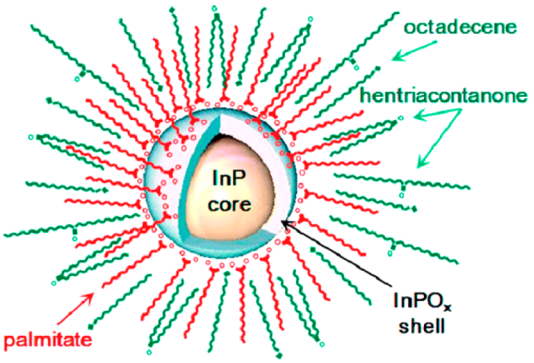

$$2CH_3(CH_2)_{14}COOH \xrightarrow{\text{InP QDs,300°C}} [CH_3(CH_2)_{14}]_2CO + H_2O + CO_2$$

Figure 8. Schematic view of InP NCs obtained by the reaction of indium palmitate with $P(SiMe_3)_3$ in ODE (top) and ketonization reaction generating hentriacontanone (palmitone) and water (bottom). Reproduced with permission from ref 81. Copyright 2010 American Chemical Society.

This side reaction is undesired as water creates an oxidative environment that leads to partial oxidation of the surface of the InP NCs, forming an InP/InPO$_x$ core/shell structure. This oxidation layer influences the optical properties of the InP NCs and likely impedes further nanocrystal or shell growth. The growth limiting role of water in the reaction medium has been confirmed by a study of Xie et al. which showed that with a low water:indium myristate ratio of 0.015 the size of InP NCs could be tuned with reaction time and temperature enabling to shift the excitonic peak to 620 nm, while with a ratio of 0.142 it stagnated at 550 nm.[83] It should be noted that the decomposition of fatty acids is not the only source of water contamination. First, indium acetate, generally used for the preparation of indium myristate or palmitate, can contain water. Second, if amines are present in the reaction mixture, their condensation reaction with carboxylic acids can also lead to water formation (see below).

In a study using ^{31}P NMR and UV−vis spectroscopy Cossairt et al. showed that the carboxylic acid ligand influences the precursor conversion of $P(SiMe_3)_3$ as it opens up an acid catalyzed reaction pathway converting $P(SiMe_3)_3$ to $(Me_3Si)_nPH_{3-n}$.[84] Importantly, this protonolysis takes place on a faster time scale than NC formation and therefore interferes with the standard $P(SiMe_3)_3$ conversion. The resulting unstable monomer supply has been suggested to be at the origin of the comparably broad InP NCs' size distribution. Limiting the amount of free acid in the reaction mixture is therefore of high importance. As has been shown earlier by Narayanaswamy et al.,[85] the in situ preparation of indium myristate from indium acetate and myristic acid in ODE does not obligatorily lead to In(MA)$_3$. Based on FTIR analyses it was proposed that when the indium acetate:myristic acid ratio was set to 1:3 the resulting indium complex contained two myristate and one acetate ligand. Therefore, the presence both of acetate ligands and of free myristic acid has to be taken into account when developing synthesis methods for InP NCs using this indium precursor. Meanwhile the preparation of indium myristate has gathered more attention and optimized procedures have been proposed, which after purification lead to the nominal In(MA)$_3$ stoichiometry with no free extra acid and/or acetate.[86]

4.2. Role of Amines. The addition of alkylamines to reactions between indium carboxylate and $P(SiMe_3)_3$ has a strong influence on the reaction mechanism and the optical properties of the obtained InP NCs. Both "activation" and "inhibition" of the reaction have been reported upon amine addition, which is likely due to the different temperatures at which the corresponding studies have been conducted. Initially, it was suggested that the mildly protic amine hydrolyzes $P(SiMe_3)_3$ thereby activating the reaction.[9,87] Indeed, the addition of oleylamine to the "standard" procedure using indium myristate and $P(SiMe_3)_3$ in ODE enables lowering the reaction temperature from 300 °C to 250−270 °C.[87] Unfortunately, in this temperature range the simultaneous presence of carboxylic acids and primary amines can lead to the formation of amides accompanied by the in situ formation of water. This small amount of water triggered the growth of an In_2O_3 shell on the InP surface.[88] The latter can improve the PL QY with respect to the core (<1%) to values of 6−8% but is problematic in view of further improvement to higher values. When applying a much shorter amine (octylamine), injected together with $P(SiMe_3)_3$ into the hot In precursor solution, Peng and co-workers achieved the formation of high quality InP QDs at significantly lower reaction temperature (≈190 °C).[87] The authors propose that short chain primary amines act as activators for the reaction. The decrease of the reaction temperature also diminishes the tendency for undesired In_2O_3 formation although the condensation reaction between carboxylic acids and amines can occur even at lower temperatures (160 °C).[89] Another appealing feature of this method is the fact that the emission could be tuned in a range of 450−750 nm, while without amine addition it was not possible to reach wavelengths beyond 590 nm. Subsequently Bawendi and co-workers studied the role of 1-octylamine in the synthesis of InP NCs.[60] To do so, the temporal evolution of the ^{1}H NMR spectra at 40 °C was monitored. The first interesting finding was that despite the low temperature formation of InP NCs takes place, albeit of lower crystalline quality. Increasing the amount of amine was found to slow down the precursor decomposition. In the conditions of Peng's synthesis,[87] namely, with an amine excess of a factor 6 with respect to indium myristate, after 10 min at 40 °C still around 40% of $P(SiMe_3)_3$ is present. The reaction mechanism depicted in Scheme 2 was derived from these studies. Therefore, primary amines such as octylamine likely acted as "reaction inhibitors" at low

Scheme 2. Mechanism for InP NC Formation in the Presence of Octylamine Derived from ^{1}H NMR Studies Conducted at Low Temperature (40°C)[a]

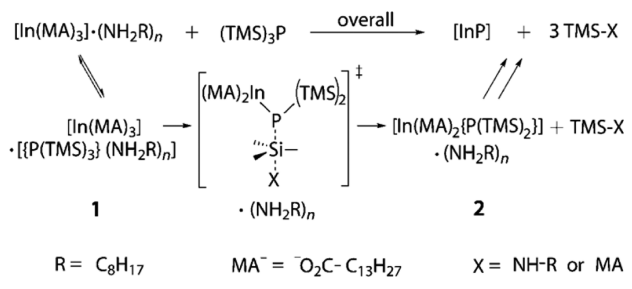

[a]Reproduced with permisison from ref 60. Copyright 2010 Wiley VCH.

DOI: 10.1021/acs.chemmater.5b05044
Chem. Mater. 2016, 28, 2491−2506

temperatures and as "reaction activators" at elevated temperatures.

A recent study of Cossairt and co-workers shed more light on the role of amines.[68] Reacting $P(SiMe_3)_3$ and indium myristate under identical experimental conditions as Peng's synthesis[87] but without addition of octylamine led to the formation of magic-sized clusters (MSCs, cf. Section 3). These were found to be kinetically persistent at $T < 120$ °C and to undergo heterogeneous growth under destabilization of the MSCs to around 3 nm InP QDs at $T > 150$ °C. When carrying out the same reaction while adding octylamine, homogeneous growth of InP QDs with no signs of the formation of MSCs has been observed, and NCs of several distinct sizes could be isolated. Homogeneous growth took place also when adding octylamine to a reaction mixture containing preformed InP MSCs. In view of these results, it can be concluded that the main effect of amines is to destabilize MSCs or to prevent their formation, a role that is coherent with the fact that they can both inhibit precursor conversion at lower temperatures and accelerate the reaction at higher temperatures.

4.3. Role of Zinc Carboxylates. Several groups have reported the beneficial effect of adding zinc carboxylates (e.g., zinc undecylenate, zinc stearate, or zinc acetate) to the reaction mixture on the optical properties of the resulting InP NCs, in particular on their PL QY. In principle, zinc carboxylates containing long alkyl chains like zinc stearate or zinc oleate can have two roles, depending on the reaction conditions: first, as Lewis acids they can act in form of Z-type surface ligands, completing for example the coordination sphere of surface phosphorus atoms and passivating trap states;[90] second, they can serve as zinc source during the reaction, leading to the formation of alloyed InZnP NCs.[91] Li et al. reported on the addition of zinc stearate to a crude solution of InP NCs and found that subsequent heating to 250 °C drastically increased the PL QY, which was attributed to an improved surface passivation of phosphorus dangling bonds by zinc carboxylate.[13] Nann and co-workers have shown that synthesizing InP NCs in the presence of zinc undecylenate and hexadecylamine dramatically increased the PL efficiency (~30%).[9] They hypothesized that zinc carboxylate and hexadecylamine both act as ligands improving the surface passivation of the obtained InP NCs. In both cases, the zinc carboxylates play the role of a neutral Z-type acceptor, while in the second example hexadecylamine acts as a neutral L-type donor according to the covalent bond classification method. A similar observation of PL enhancement was reported with the addition of zinc acetate.[92] Here another role has been attributed to the zinc carboxylate in addition to eventual surface passivation, namely, surface etching of the InP NCs by *in situ* generated acetic acid. To elucidate the effect of zinc stearate added *initially* to the reaction mixture (i.e., before heating to elevated temperature), Thuy et al. utilized a combination of powder XRD, UV−vis absorption, steady-state and time-resolved photoluminescence (TRPL) spectroscopy providing strong evidence that the altered optical properties of the obtained InP NCs were rather due to incorporation of zinc in the InP lattice than to enhanced surface passivation by zinc carboxylates.[91] In particular, it was observed that samples prepared in the presence of zinc stearate showed a much larger Stokes shift than samples without (370 meV vs 280 meV for samples with Zn:In ratios of 1:1 and 0:1, respectively). This was rationalized in terms of band edge fluctuations due to the formation of an InZnP alloy, enhancing the confinement of the excited charge carriers. TRPL studies corroborated this hypothesis: The PL signal was found to decay with two time constants (38 and 85 ns for a Zn:In ratio of 1:1), the shorter one being attributed to recombination at surface states, the longer one to excitonic recombination. With increasing Zn concentration the decay times of both emission mechanisms increased. This behavior is in accordance with an enhanced confinement of the excited carriers by lattice fluctuations induced by the higher Zn contents. Additionally, it was shown that by varying the In^{3+}:Zn^{2+} ratio, the emission of In(Zn)P/ZnS alloyed core/shell NCs could be tuned from 485 to 586 nm. Be it for improving the surface passivation or for adapting the lattice parameter through alloying, currently most of the InP NCs syntheses make use of a certain amount of zinc carboxylates added in the beginning of the reaction with typical Zn:In molar ratios of 0.5−1.

4.4. Adding the In Precursor after Nanocrystal Synthesis: Cation Exchange. A novel approach for obtaining InP NCs starting from completely different materials is cation exchange. Thermodynamically driven cation exchange reactions are well-documented in II−VI semiconductor nanocrystals,[93] while in the case of III−V compounds it has first been realized by Beberwyck and Alivisatos in 2012.[94] In their study they converted Cd_3P_2 NCs into InP by the addition of $InCl_3$ and trioctylphosphine (TOP) and heating to 300 °C. As the diffusivity of ions in the more covalent III−V systems is much lower than in the more ionic II−VI compounds, residual Cd concentrations of a few atomic percent remain in the exchanged samples. Also, the reaction has to be carried out at high temperature, while in the II−VI systems many exchange reactions take place at room temperature. Another recent example is the transformation of hexagonal $Cu_{3-x}P$ nanoplatelets of 10−50 nm diameter into InP NCs of the same shape in the metastable wurtzite phase.[95] The cation exchange reaction uses a solution of $InBr_3$ and TOP in ODE at 200 °C, to which the colloidal solution of $Cu_{3-x}P$ NCs in ODE is added (In:Cu molar ratio 1:1). The reactions used in these examples can be formulated as follows:

$$M_x^{n+}P_y + y\mathrm{InX_3} \xrightarrow{\mathrm{TOP},\Delta} y\ \mathrm{ln\ P} + x\mathrm{MX}_n \quad (\mathrm{X = Cl, Br})$$

A limitation of the cation exchange approach could be that so far in InP NCs obtained by this method no photoluminescence could be detected. Recently, InP NCs have been coated with GaP via cation exchange, which led to an increase in the PL QY.[14] InP/GaP/ZnS core/shell/shell NCs with a QY of up to 85% have been reported with this method.

5. CORE/SHELL SYSTEMS

As-synthesized InP NCs exhibit generally poor fluorescence QYs of less than 1% and are prone to photodegradation and surface oxidation. Overcoating the NCs with a shell of a larger band gap semiconductor is a common method for enhancing the PL efficiency and improving at the same time the photo- as well as chemical stability. Three physical parameters have to be considered when selecting an appropriate shell material: (a) the band gap of the shell material, which should be significantly larger than that of the core in order to provide efficient charge carrier confinement in the core; (b) the relative position of the conduction and valence band of the two materials (band alignment)—ideally the offsets should be large for both the valence band and conduction band edges; (c) the crystal structures and lattice parameters of the core and shell materials, which should be as close as possible in order to facilitate

DOI: 10.1021/acs.chemmater.5b05044
Chem. Mater. 2016, 28, 2491−2506

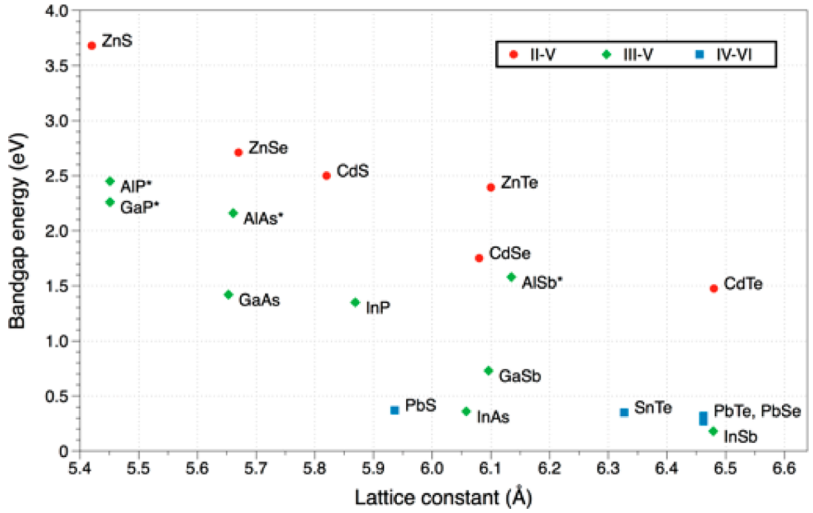

Figure 9. Band gap energies and lattice parameters of various semiconductors used as core or shell materials in colloidal nanocrystals (* indicates indirect band gap materials).

epitaxial-like growth of the shell material on the core NCs. The band gap values and lattice parameters for many materials used in semiconductor NCs are depicted in Figure 9, while a diagram showing the band alignment of these semiconductors can be found in ref 96.

Depending on the band alignment of the core and shell materials, NCs can be type I or type II. In a type I core/shell system the conduction band edge of the shell (the higher band gap material) is of higher energy than that of the core (the lower band gap material), and the valence band edge of the shell has lower energy than that of the core. Consequently, both electrons and holes are confined in the core.[7] InP/ZnS NCs[7,9,13,87,97] are the most commonly synthesized InP based type I structure. Other examples are InP/ZnSe,[98] InP/$ZnCdSe_2$,[99] and InP/ZnSeS.[100] In a type-II QD in contrast, both the valence and conduction band edges in the core are situated below or above the corresponding band edges of the shell. As one carrier is confined to the core, and the other is confined to the shell, the PL emission of type II systems is red-shifted. As a result, longer emission wavelengths are accessible than with both individual materials.[101] An example of an InP based type II structure is InP/CdS.[102]

Concerning the minimization of crystallographic strain in InP-based core/shell systems, the earliest attempt was the synthesis of lattice-matched InP/$ZnCdSe_2$.[99] However, although a shell thickness up to 5 nm could be achieved, the PL QY of the InP/$ZnCdSe_2$ core/shell NCs was only increased up to 5−10%. Haubold et al. synthesized for the first time InP/ZnS core/shell NCs and despite the lattice mismatch of 7.7% between core and shell, a QY of about 20% was achieved. The shell thickness was measured to be around 0.5 nm, i.e. the equivalent of 1−2 monolayers of a ZnS shell.[97] This trend of superior photoluminescence efficiency but limitation to a thin shell (<1 nm) imposed by lattice strain is a common observation in InP/ZnS core/shell QDs.[9,13,97] The fact that shell growth is possible at all despite the large lattice mismatch between InP and ZnS can be attributed to the relaxation of strain in small nanocrystals with short facets. Nevertheless thicker shells (>3 monolayers) would be desired because these allow improved photo- and air-stability of the core.[96] On the other hand, in the case of CdSe/ZnS NCs lattice mismatch between core and shell is even larger (10−11%) but thicker shells (up to ≈4 monolayers) have been grown successfully.[103] As already mentioned above, the *in situ* formation of an oxidized surface state in the case of InP may be at the origin of these differences (cf. Figure 8).[81,82] Therefore, in case of high temperature (>250 °C) syntheses implying indium carboxylate precursors, the *in situ* formed interfacial oxide layer is a plausible explanation for the failure of growing thicker ZnS shells on InP QDs.

Recently, alternative ways to alleviate lattice strain have been proposed. One approach incorporates zinc into the InP core leading to InZnP alloy NCs,[91] which show a PL QY of up to 70% after overcoating with a ZnS shell. Other works make use of a so-called lattice adaptor, i.e., a material of intermediate lattice constant used at the interface between core and shell. This approach has been successfully applied to II−VI NCs where ZnSe or CdS can play the role of an intermediate layer between the CdSe core and the ZnS outer shell. Lim and co-workers have used ZnSe, which has lower lattice mismatch (3.3%) with InP, as a lattice adaptor to achieve thicker ZnS shells.[100] Although according to the authors only a submonolayer (≈0.6 monolayers) of ZnSe has been achieved on the InP core, 4.5 monolayers of ZnS could be grown on top. The resulting InP/ZnSeS NCs showed high PL QY of around 45% and improved photostability.[100,104] It should be noted that the distinction between a core/shell/shell structure and a compositional gradient is not easy to be made in this case.[100] More recently GaP has been employed as intermediate layer even though its lattice mismatch parameter (7%) is almost the same as for ZnS (cf. Figure 9).[14] In this case cation exchange has been applied to replace around 10−15% of In with Ga, presumably at the NC surface. The diameter remained essentially unchanged during this step (3.1 nm before, 3.3 nm after cation exchange). After growth of a 0.7 nm thick ZnS shell, the obtained InP/GaP/ZnS NCs showed the highest QY reported so far (maximum QY 85%) and superior photostability as compared to InP/ZnS NCs. As in the case of other materials families, for a given combination of core and shell materials, the PL QY goes through a maximum corresponding to the optimum thickness and decreases with further shell growth due to the strain-induced formation of structural defects.[105] The intermediate shell materials like ZnSe (or GaP) show a reduced offset of the conduction band (valence band) as

DOI: 10.1021/acs.chemmater.5b05044
Chem. Mater. 2016, 28, 2491−2506

Table 2. Synthesis Methods for ZnS Shells on InP-Based NCs

system	shell precursors	temp.	time	thickness	QY_{max}	ref
InP/ZnS	zinc diethyldithiocarbamate	230 °C	20 min	not spec.	60%	9
InP/ZnS	Zn-stearate/dodecanethiol	230 °C ~ 300 °C	5 min−2 h	0.6−1 nm	70%	13
InP/ZnSeS	TOPSe, S(TBT), Zn-oleate, dodecanethiol	280 °C	~90 min	1.1 nm	80%	100
InP/ZnSe/ZnS	(1) TOPSe, S(TBT), Zn-oleate, dodecanethiol	(1) 280 °C	(1) 90 min	1.7 nm	70%	104
	(2) Zn-oleate, dodecanethiol	(2) 300 °C	(2) 2 h			
InP/GaP/ZnS	(1) $GaCl_3$	(1) 200 °C	(1) 4 h	1.9 nm	85%	14
	(2) Zn-acetate, dodecanethiol	(2) 230 °C	(2) 2 h			

compared to ZnS, hence the confinement of the electron (hole) in the core is less pronounced. This translates in a red-shift of the emission spectrum during shell growth, which has to be taken into account when fluorescence at a precisely determined wavelength is desired.

A former review on core/shell NCs covers the main aspects of shell synthesis such as the choice of precursors and reaction parameters for different combinations of materials.[96] We focus here our attention on ZnS as the (outer) shell material, which is the most widely used one combining nontoxicity, chemical stability, low cost, and wide band gap (3.6 eV). A number of different methods for ZnS shell growth, with or without additional intermediate shell, are summarized in Table 2. Successful synthesis of core/shell NCs requires that the shell material grows on the surface of the core rather than in form of separate NCs in solution. In order to prevent separate homogeneous nucleation usually shell synthesis is carried out at lower temperatures than core synthesis and in diluted regime, e.g. through the dropwise injection of the shell precursors. In their initial synthesis, Haubold et al. used the highly reactive organometallic precursors diethylzinc (Et_2Zn) and bis(trimethylsilyl)sulfide ($S(SiMe_3)_2$) to grow ZnS on InP NCs. Nonetheless a relatively high temperature of 260 °C was required for initiating the reaction. In order to avoid Ostwald ripening of InP as well as separate ZnS nucleation, the heating at this temperature was kept as short as possible.[98] In the following, the initial pyrophoric precursors have been replaced with easier to handle, more stable precursors such as zinc carboxylates (e.g., zinc stearate or zinc oleate) and elemental sulfur dissolved in appropriate Lewis bases (e.g., TOP, oleylamine).

Dodecanethiol (DDT) has also been proposed as sulfur source for the shell and applied in a one-pot heat-up method yielding InP/ZnS NCs with a maximum QY of 70%.[13] The high fluorescence QY is attributed to an alloyed InPZnS core overcoated with a thin ZnS layer, leading to nearly defect-free core/shell NCs.[106] Another class of compounds suitable for ZnS shell growth are monomolecular precursors combining both the zinc and sulfur source in one molecule. Li et al. used for example zinc ethylxanthate,[65] while Xu et al. synthesized highly luminescent InP/ZnS NCs (QY ~ 60%) applying zinc diethyldithiocarbamate.[9] The ratio of Zn:S in zinc ethylxanthate is 1:4 and therefore zinc stearate is usually added to compensate the shortage of zinc.[107] The interest in using monomolecular precursors for ZnS shell growth stems from the following advantages: (a) they are easy to synthesize and to handle; (b) they are generally air stable; (c) shell growth using these compounds is simpler than thermal cycling[87] or multiple injection approaches (SILAR)[108] used with separate precursors; (d) their low decomposition temperature, generally below 200 °C.[109] Xi et al. have studied the effect of different substitutions on zinc dithiocarbamate based monomolecular precursors on the reaction temperatures and the QY of the obtained InP/ZnS NCs.[109] They found that compounds with bulky substituents (benzyl) result in NCs of higher PL QY and better dispersibility in organic solvents than those synthesized with precursors containing shorter alkyl chains (methyl, ethyl, butyl). Concluding this section, careful optimization of the synthesis parameters has led to InP-based core/shell systems with a PL QY approaching unity. In addition, their thermal stability of emission is higher, i.e. thermal PL quenching is lower than in the case of II−VI QDs: with InP-based QDs QYs > 70% have been observed up to 175 °C, while with CdSe based NCs a significant part of the initial emission intensity is lost when exceeding 120 °C.[110] These features, together with their intrinsic less-toxic nature has heralded InP based NCs as one of the potential materials for solid-state lighting applications.[104]

6. DOPED InP NANOCRYSTALS

Controlled and intentional insertion of impurity atoms into a semiconductor crystal in bulk form, also known as doping, has an enormous importance in the application of semiconductor materials in electronic devices. On the contrary, doping in quantum dots (d-QDs) and in particular in III−V QDs is still in its formative stage.[111] The reason for this lies in the synthetic challenge of incorporating impurity atoms into the lattice of the NCs as compared to the mere adsorption on their surface.[112] Furthermore, bringing up the unambiguous evidence for successful lattice doping and distinguishing between substitutional and interstitial doping are challenging tasks in NC research. The efforts on NC doping are mainly driven by the following possibilities: (a) based on the electron donating or accepting ability of the impurity, n-type or p-type materials can be synthesized; (b) doping can be used to tune the optical, electrical and magnetic properties of the QDs; (c) the toxicity problems can be addressed by achieving the desired optical properties with less-toxic materials; (d) doping may also enhance the chemical and thermal stability of the NCs and their emission properties.[113,114] Copper doping of InP QDs has first been demonstrated by Xie and Peng who achieved tunable emission in the red and NIR regions (630−1100 nm).[115] This is a significant enlargement of the spectral range of emission, as without doping no emission beyond 750 nm has been reported. The added Cu^{2+} ions introduce electronic acceptor states within the band gap of InP, which results in optical transitions at lower energy/higher wavelength. Reaction temperature was found to be a key element for the successful doping. The copper precursor (copper(II) stearate) was added at 130 °C to the preformed InP NCs, enabling effective surface adsorption of the dopant ions. Subsequently the temperature was increased to 210 °C at a rate of 2 °C/min to induce diffusion and lattice incorporation. Gamelin and co-workers investigated this type of d-QDs by means of magnetooptical measurements and demonstrated that in the ground state, the copper dopant is

DOI: 10.1021/acs.chemmater.5b05044
Chem. Mater. 2016, 28, 2491−2506

in its +1 oxidation state.[116] Upon photo-oxidation, fast nonradiative hole transfer from the InP valence band to the copper dopant takes place, resulting in a Cu^{2+}-like ion, which then radiatively recombines with an electron from the conduction band. Xie and co-workers took advantage of the red-shifted emission of the Cu-doped InP QDs to synthesize dual-emitting InP:Cu/ZnS/InP/ZnS multishell NCs.[117] The successive ionic layer adsorption and reaction (SILAR) technique was used to precisely control shell thicknesses and hence optical properties.[118] Here the intermediate ZnS shell separates the inner InP:Cu NC emitting at 600−800 nm from an outer InP quantum well emitting at 480−600 nm. The lifetime of the transition involving the dopant states is approximately 1 order of magnitude longer (500 ns) than that of the InP quantum well (46 ns) and the PL QY of the combined emission has been estimated as 35%. Another successful example of InP QD doping was achieved by using Eu^{3+} as the dopant.[119] The isovalent Eu^{3+} atoms do not introduce free carriers or new electronic states in the band gap of InP. However, if the host QDs are chosen small enough (blue-emitting), they can serve as an antenna for sensitizing the lanthanide emission through charge or energy transfer. Eu-oleate was used as the Eu source and the steps of dopant adsorption and lattice incorporation were carried out at 80 and 120 °C, respectively, before overcoating the Eu-doped NCs with a ZnS shell. Maximum Europium phosphorescence efficiency was achieved with a Eu^{3+}:In^{3+} molar ratio of 0.3:1 used during synthesis corresponding to an effective doping level of approximately 4%.

7. INDIUM PHOSPHIDE AS PROTOTYPE FOR THE SYNTHESIS OF OTHER III−V SEMICONDUCTOR NCs

The progress in the synthesis of InP NCs described in the previous sections is expected to be very beneficial also for the development of other III−V semiconductor QDs including InAs, GaAs, InSb, etc. with similar bonding nature. The fractional ionic character of InAs (0.36) and InSb (0.32) are similar to InP (0.42) and representative of much more covalent bonding as compared to CdSe (0.70).[120] In parallel to the use of $P(SiMe_3)_3$ as phosphorus source $As(SiMe_3)_3$ has been applied in the synthesis of InAs NCs. As an example, Alivisatos and co-workers have synthesized InAs QDs in TOP as both coordinating ligand and solvent by reacting $As(SiMe_3)_3$ and $InCl_3$.[121] Peng and co-workers have developed synthetic schemes for high quality InAs NCs in 1-octadecene using fatty acids as capping ligands.[11] As expected the problems associated with InP NCs synthesis are also relevant for InAs NCs. In particular, due to the rapid depletion of $As(SiMe_3)_3$ the synthesis of larger sized InAs QDs typically requires the secondary injection of the As precursor followed by size selective precipitation.[121] The dehalosilylation approach has also been extended to InSb NCs, albeit with limited success due to the very high reactivity and sensitivity of $Sb(SiMe_3)_3$.[122] Similarly, following the successful synthesis of InP NCs using PH_3 as the phosphorus source in a noncoordinating solvent,[65] AsH_3[123] as well as SbH_3[124] have been used for the synthesis of InAs and InSb, respectively. These examples demonstrate the successful cases of direct translation of InP NCs synthesis methods to InAs and InSb. On the other hand, the control of size and size distribution of InSb NCs turned out to be more challenging using these approaches as compared to InP and InAs NCs. Talapin and co-workers proposed another synthetic scheme relying on the coreduction of $Sb(N(SiMe_3)_2)_3$ and $InCl_3$ by means of $LiEt_3BH$ (superhydride) in a solvent mixture of dioctyl ether, oleylamine and TOP, yielding InSb QDs exhibiting size-dependent optical properties.[125] Superhydride has been found to be crucial for generating $In^{(0)}$ and $Sb^{(0)}$ species, which are expected to be reaction intermediates and for providing a reductive environment preventing from oxidative side reactions. Despite of the successful use of $P(NMe_2)_3$ as phosphorus source in the synthesis of InP NCs, similar attempts to synthesize InSb by reacting $Sb(NMe_2)_3$ with $InCl_3$ failed.[126,127] Yarema et al. found that the commonly employed ionic indium precursors like $InCl_3$ or In acetate were not reactive enough in combination with $Sb(NMe_2)_3$ to form InSb NCs. On the other hand, the covalent precursor Me_3In led to the uncontrolled formation of aggregated and polydisperse InSb NCs. Indium silylamide, $In(N(SiMe_3)_2)_3$, with polar In-N bonds was found to be the optimum choice, giving access to InSb NCs of comparably low size distribution whose excitonic peak position could be tuned from 1250 to 1750 nm by changing the NC size.[126] Furthermore, depending on the solvent used (TOP or trioctylamine) and In:Sb precursor ratio, NCs in the zinc blende or wurtzite crystal structure have been obtained, the latter enabling the formation of anisotropic shapes (nanorods).

8. CONCLUSIONS AND PERSPECTIVES

The significant progress made in the last 15 years in the chemical synthesis of InP-based NCs has brought their optical properties to a quality comparable to established II−VI and IV−VI QDs. As a matter of fact, their integration into commercial optoelectronic devices, in particular in the display sector, is currently developed. Still further progress needs to be made, in particular in identifying synthetic schemes allowing for a decrease of the size distribution at high reaction yield and for achieving a precisely controlled, predefined emission wavelength with enhanced stability. As highlighted in this article, the identification of appropriate precursors and reaction conditions for achieving these goals is much more challenging than with more ionic semiconductor families. In the following we list the directions of research, which we consider most promising for improving the synthesis of InP QDs:

(1) One persisting drawback in the synthesis of InP NCs is the low availability of suitable phosphorus precursors. $P(SiMe_3)_3$ has been the most widely used so far, but LaMer like growth of monodisperse NCs is precluded due to the very fast depletion of this precursor in the early stages of the reaction, implying that growth occurs predominantly via Ostwald ripening.[86] As predicted by kinetic models and verified experimentally for metal chalcogenide NCs, a high monomer concentration must be present during the growth stage in order to be able to achieve size focusing.[59] Despite of enforcing LaMer like growth of InP NCs by using simultanously two types of silylphosphine precursors of different reactivity, the size dispersion could not be improved.[54] Attempts to tune the conversion rates of phosphorus sources by replacing silylphosphines by germylphosphines also met with limited success.[53] While varying the precursor-to-monomer conversion rate is in case of II−VI and IV−VI semiconductor NCs an efficient means for tuning the synthesis toward minimum size dispersion under full reaction yield,[48] this strategy could not be exploited successfully in the case of InP NCs.[52] However, recently promising alternatives to alkyl- or arylsilylphosphines have been proposed, namely dialkylaminophosphines $P(NR_2)_3$ (R = Me,Et).[77,79,80] Their lower reactivity allows for an

DOI: 10.1021/acs.chemmater.5b05044
Chem. Mater. 2016, 28, 2491−2506

improved fine-tuning of the reaction kinetics, which should ultimately give access to InP NCs of reduced size distribution without the requirement of postsynthetic size selection processes.

(2) While most recent studies focus on the conversion kinetics of the P precursor, very few studies address the chemical transformations of the indium precursor in the course of the reaction. Only recently, theoretical studies have been performed to understand the short-lived intermediates at the early stage of the growth of InP NCs.[128] Using high-temperature *ab initio* molecular dynamics (AIMD) simulation, Kulik and co-workers have reported the early stage formation of In-rich clusters. The cluster formation between $In(Ac)_3$ and PH_3 involved agglomeration of individual Indium precursor molecules into an $[In(Ac)_3]_6$ complex which subsequently formed an adduct with PH_3. The dissociation of P−H bonds with simultaneous formation of In−P bonds marked the evolution of InP clusters with structural properties similar to bulk zinc blende.[128] This study clearly underlines the role of reactivity of the indium precursor by influencing the energetics of the reaction pathways of InP formation. While indium myristate, prepared from indium acetate and myristic acid, has been used for many years,[11] only very recent studies focus on the importance of the preparation conditions and on the impact of free myristic acid on the reaction mechanism.[83,84] This underlines that in-depth *in situ* (e.g., UV−vis absorption) and *ex situ* (e.g., liquid phase and solid-state NMR, XPS, electron microscopy) studies are of prime importance for the design of efficient synthesis methods,[68,82,106] as they provide the necessary insight into precursor conversion kinetics, eventual side-reactions, internal structure and surface state of the obtained NCs.

(3) Most of the current strategies are based on maintaining a high monomer concentration during growth internally by controlling the reactivity of the precursors. Supplying additional precursors externally during the growth stage, either by multiple or continuous injection, is a promising yet underexplored alternative. As one example a synthesis using continuously supplied PH_3 gas gave access to larger sized InP NCs without sacrificing the size distribution.[65] Another way to maintain a high monomer reservoir could be the use of suitable complexing agents that enhance the stability of molecular precursors *in situ*.

(4) In most nucleation and growth studies the pure crystalline phase of bulk InP is assumed. However, there are many instances, where the formation of an amorphous phase was observed before the evolution of the crystalline phase, affecting the energetics of nucleation and growth.[129] Interestingly, both experimental[81] and theoretical studies[130] have revealed that partially oxidized InP surfaces are amorphous in nature. In this context it has been demonstrated that the presence of traces of water or hydroxide impurities limit the size tunability.[83]

(5) The recent observation and isolation of MSCs is very promising and may hold the key for further improving the quality of III−V nanocrystals.[68,76] Besides the insight gained on the early stages of NC growth, structural properties of small InP clusters and surface ligand coordination modes, MSCs can also be explored as single molecular precursors that can provide a controlled monomer reservoir for the nucleation and growth stages.

(6) Engineering of core/shell structures for reaching maximum PL QY and chemical and photostability remains a challenging task. Graded (ZnSe,S) shells and the use of a thin GaP intermediate layer have been demonstrated to offer promising perspectives in this direction.[14] Improved understanding of surface/interface passivation would benefit designing core/shell structures with tuned optical properties. Finally, in view of the large-scale production of InP NCs, further aspects related to the availability of precursors, stabilizers and solvents and to the sustainability of the syntheses have to be considered.

(7) Very few works exist on the doping of InP-based NCs, which demonstrate nonetheless the potential of this approach for introducing a further way for tuning their optical and electronic properties. So far the control of the doping has not reached the same level as with for CdSe NCs, where Norris and co-workers were able to add Ag^+ dopants "one-by-one" and showed tremendous effects on the emission properties.[112] Another concept not yet explored is shell-doping, i.e., introduction of the dopant ions into the shell material, which gives additional degrees of freedom based on established methods for doping ZnSe and ZnS.

Concluding, the field of InP-based QDs has (re)gained a significant research interest within the past few years. The recent developments highlighted in this article illustrate the rapid progress both in the fundamental understanding of the underlying chemistry and in the improvement of the optical properties of the obtained InP NCs. We expect that the knowledge gained with InP will have strong impact also on the synthesis of other metal pnictide QDs, further enlarging the palette of high quality luminescent NCs.

AUTHOR INFORMATION

Corresponding Authors

*(S.J.) E-mail: sjeong@kimm.re.kr.
*(P.R.) E-mail: peter.reiss@cea.fr.

Notes

The authors declare no competing financial interest.

ACKNOWLEDGMENTS

P.R. and C.L. acknowledge financial support from the French Research Agency ANR (Grant Numbers ANR-13-BS08-011-03 NIRA, ANR-12-NANO-0007-03 NanoFRET). S.T. and S. J. were supported by the Global Frontier R&D program by the Center for Multiscale Energy Systems (2011-0031566) and the Global R&D program (1415134409) funded by KIAT. S.T. also acknowledges Sikkim University for support.

REFERENCES

(1) Ekimov, A. I.; Efros, A. L.; Onushchenko, A. A. Quantum size effect in semiconductor microcrystals. *Solid State Commun.* **1985**, *56*, 921−924.

(2) Efros, A. L. Interband Absorption of Light in a Semiconductor Sphere. *Soviet Physics Semiconductors USSR* **1982**, *16*, 772−775.

(3) Rossetti, R.; Brus, L. Electron-hole recombination emission as a probe of surface chemistry in aqueous cadmium sulfide colloids. *J. Phys. Chem.* **1982**, *86*, 4470−4472.

(4) Alfassi, Z.; Bahnemann, D.; Henglein, A. Photochemistry of colloidal metal sulfides. 3. Photoelectron emission from cadmium sulfide and cadmium sulfide-zinc sulfide cocolloids. *J. Phys. Chem.* **1982**, *86*, 4656−4657.

(5) Rossetti, R.; Nakahara, S.; Brus, L. E. Quantum size effects in the redox potentials, resonance Raman spectra, and electronic spectra of CdS crystallites in aqueous solution. *J. Chem. Phys.* **1983**, *79*, 1086−1088.

DOI: 10.1021/acs.chemmater.5b05044
Chem. Mater. 2016, 28, 2491−2506

(6) Murray, C. B.; Norris, D. J.; Bawendi, M. G. Synthesis and characterization of nearly monodisperse CdE (E = sulfur, selenium, tellurium) semiconductor nanocrystallites. *J. Am. Chem. Soc.* **1993**, *115*, 8706−8715.
(7) Hines, M. A.; Guyot-Sionnest, P. Synthesis and Characterization of Strongly Luminescing ZnS-Capped CdSe Nanocrystals. *J. Phys. Chem.* **1996**, *100*, 468−471.
(8) Talapin, D. V.; Rogach, A. L.; Kornowski, A.; Haase, M.; Weller, H. Highly luminescent monodisperse CdSe and CdSe/ZnS nanocrystals synthesized in a hexadecylamine-trioctylphosphine oxide-trioctylphospine mixture. *Nano Lett.* **2001**, *1*, 207−211.
(9) Xu, S.; Ziegler, J.; Nann, T. Rapid synthesis of highly luminescent InP and InP/ZnS nanocrystals. *J. Mater. Chem.* **2008**, *18*, 2653−2656.
(10) Reiss, P.; Bleuse, J.; Pron, A. Highly Luminescent CdSe/ZnSe Core/Shell Nanocrystals of Low Size Dispersion. *Nano Lett.* **2002**, *2*, 781−784.
(11) Battaglia, D.; Peng, X. Formation of High Quality InP and InAs Nanocrystals in a Noncoordinating Solvent. *Nano Lett.* **2002**, *2*, 1027−1030.
(12) Hines, M. A.; Scholes, G. D. Colloidal PbS nanocrystals with size-tunable near-infrared emission: Observation of post-synthesis self-narrowing of the particle size distribution. *Adv. Mater.* **2003**, *15*, 1844−1849.
(13) Li, L.; Reiss, P. One-pot Synthesis of Highly Luminescent InP/ZnS Nanocrystals without Precursor Injection. *J. Am. Chem. Soc.* **2008**, *130*, 11588−11589.
(14) Kim, S.; Kim, T.; Kang, M.; Kwak, S. K.; Yoo, T. W.; Park, L. S.; Yang, I.; Hwang, S.; Lee, J. E.; Kim, S. K.; Kim, S.-W. Highly Luminescent InP/GaP/ZnS Nanocrystals and Their Application to White Light-Emitting Diodes. *J. Am. Chem. Soc.* **2012**, *134*, 3804−3809.
(15) Talapin, D. V.; Steckel, J. Quantum dot light-emitting devices. *MRS Bull.* **2013**, *38*, 685−691.
(16) Green, M. Solution routes to III-V semiconductor quantum dots. *Curr. Opin. Solid State Mater. Sci.* **2002**, *6*, 355−363.
(17) IARC. Indium Phosphide. In *Monographs on the Evaluation of the Carcinogenic Risk of Chemicals to Humans*; World Health Organization: 2006.
(18) Lin, G.; Ouyang, Q.; Hu, R.; Ding, Z.; Tian, J.; Yin, F.; Xu, G.; Chen, Q.; Wang, X.; Yong, K. T. In vivo toxicity assessment of non-cadmium quantum dots in BALB/c mice. *Nanomedicine* **2015**, *11*, 341−50.
(19) Brunetti, V.; Chibli, H.; Fiammengo, R.; Galeone, A.; Malvindi, M. A.; Vecchio, G.; Cingolani, R.; Nadeau, J. L.; Pompa, P. P. InP/ZnS as a safer alternative to CdSe/ZnS core/shell quantum dots: in vitro and in vivo toxicity assessment. *Nanoscale* **2013**, *5*, 307−17.
(20) Chibli, H.; Carlini, L.; Park, S.; Dimitrijevic, N. M.; Nadeau, J. L. Cytotoxicity of InP/ZnS quantum dots related to reactive oxygen species generation. *Nanoscale* **2011**, *3*, 2552−9.
(21) Heath, J. R. Covalency in semiconductor quantum dots. *Chem. Soc. Rev.* **1998**, *27*, 65−71.
(22) Cui, J.; Beyler, A. P.; Marshall, L. F.; Chen, O.; Harris, D. K.; Wanger, D. D.; Brokmann, X.; Bawendi, M. G. Direct probe of spectral inhomogeneity reveals synthetic tunability of single-nanocrystal spectral linewidths. *Nat. Chem.* **2013**, *5*, 602−606.
(23) Brus, L. E. Electron Electron and Electron-Hole Interactions in Small Semiconductor Crystallites - the Size Dependence of the Lowest Excited Electronic State. *J. Chem. Phys.* **1984**, *80*, 4403−4409.
(24) Narayanaswamy, A.; Feiner, L. F.; Meijerink, A.; van der Zaag, P. J. The Effect of Temperature and Dot Size on the Spectral Properties of Colloidal InP/ZnS Core−Shell Quantum Dots. *ACS Nano* **2009**, *3*, 2539−2546.
(25) Fu, H.; Zunger, A. InP quantum dots: Electronic structure, surface effects, and the redshifted emission. *Phys. Rev. B: Condens. Matter Mater. Phys.* **1997**, *56*, 1496−1508.
(26) Fan, G.; Wang, C.; Fang, J. Solution-based synthesis of III-V quantum dots and their applications in gas sensing and bio-imaging. *Nano Today* **2014**, *9*, 69−84.
(27) Mushonga, P.; Onani, M. O.; Madiehe, A. M.; Meyer, M. Indium phosphide-based semiconductor nanocrystals and their applications. *J. Nanomater.* **2012**, *2012*, 869284.
(28) Healy, M. D.; Laibinis, P. E.; Stupik, P. D.; Barron, A. R. The reaction of indium(III) chloride with tris(trimethylsilyl)phosphine: a novel route to indium phosphide. *J. Chem. Soc., Chem. Commun.* **1989**, 359−360.
(29) Wells, R. L.; Aubuchon, S. R.; Kher, S. S.; Lube, M. S.; White, P. S. Synthesis of Nanocrystalline Indium Arsenide and Indium Phosphide from Indium(III) Halides and Tris(trimethylsilyl)-pnicogens. Synthesis, Characterization, and Decomposition Behavior of I3InP(SiMe3)3. *Chem. Mater.* **1995**, *7*, 793−800.
(30) Wells, R. L.; Pitt, C. G.; McPhail, A. T.; Purdy, A. P.; Shafieezad, S.; Hallock, R. B. The use of tris(trimethylsilyl)arsine to prepare gallium arsenide and indium arsenide. *Chem. Mater.* **1989**, *1*, 4−6.
(31) Mićić, O. I.; Curtis, C. J.; Jones, K. M.; Sprague, J. R.; Nozik, A. J. Synthesis and Characterization of InP Quantum Dots. *J. Phys. Chem.* **1994**, *98*, 4966−4969.
(32) Mićić, O. I.; Nozik, A. J. Synthesis and characterization of binary and ternary III-V quantum dots. *J. Lumin.* **1996**, *70*, 95−107.
(33) Guzelian, A. A.; Katari, J. E. B.; Kadavanich, A. V.; Banin, U.; Hamad, K.; Juban, E.; Alivisatos, A. P.; Wolters, R. H.; Arnold, C. C.; Heath, J. R. Synthesis of Size-Selected, Surface-Passivated InP Nanocrystals. *J. Phys. Chem.* **1996**, *100*, 7212−7219.
(34) Yu, W. W.; Peng, X. Formation of High-Quality CdS and Other II−VI Semiconductor Nanocrystals in Noncoordinating Solvents: Tunable Reactivity of Monomers. *Angew. Chem., Int. Ed.* **2002**, *41*, 2368−2371.
(35) Liu, H.; Owen, J. S.; Alivisatos, A. P. Mechanistic Study of Precursor Evolution in Colloidal Group II-VI Semiconductor Nanocrystal Synthesis. *J. Am. Chem. Soc.* **2007**, *129*, 305−312.
(36) Steckel, J. S.; Yen, B. K. H.; Oertel, D. C.; Bawendi, M. G. On the Mechanism of Lead Chalcogenide Nanocrystal Formation. *J. Am. Chem. Soc.* **2006**, *128*, 13032−13033.
(37) Abe, S.; Čapek, R. K.; De Geyter, B.; Hens, Z. Tuning the Postfocused Size of Colloidal Nanocrystals by the Reaction Rate: From Theory to Application. *ACS Nano* **2012**, *6*, 42−53.
(38) Sugimoto, T. Preparation of monodispersed colloidal particles. *Adv. Colloid Interface Sci.* **1987**, *28*, 65−108.
(39) Kahlweit, M. Ostwald ripening of precipitates. *Adv. Colloid Interface Sci.* **1975**, *5*, 1−35.
(40) LaMer, V. K.; Dinegar, R. H. Theory, Production and Mechanism of Formation of Monodispersed Hydrosols. *J. Am. Chem. Soc.* **1950**, *72*, 4847−4854.
(41) Park, J.; Joo, J.; Kwon, S. G.; Jang, Y.; Hyeon, T. Synthesis of Monodisperse Spherical Nanocrystals. *Angew. Chem., Int. Ed.* **2007**, *46*, 4630−4660.
(42) de Mello Donega, C.; Liljeroth, P.; Vanmaekelbergh, D. Physicochemical evaluation of the hot-injection method, a synthesis route for monodisperse nanocrystals. *Small* **2005**, *1*, 1152−1162.
(43) Park, J.; An, K.; Hwang, Y.; Park, J.-G.; Noh, H.-J.; Kim, J.-Y.; Park, J.-H.; Hwang, N.-M.; Hyeon, T. Ultra-large-scale syntheses of monodisperse nanocrystals. *Nat. Mater.* **2004**, *3*, 891−895.
(44) van Embden, J.; Chesman, A. S. R.; Jasieniak, J. J. The Heat-Up Synthesis of Colloidal Nanocrystals. *Chem. Mater.* **2015**, *27*, 2246−2285.
(45) Li, C.; Ando, M.; Enomoto, H.; Murase, N. Highly Luminescent Water-Soluble InP/ZnS Nanocrystals Prepared via Reactive Phase Transfer and Photochemical Processing. *J. Phys. Chem. C* **2008**, *112*, 20190−20199.
(46) Byun, H.-J.; Lee, J. C.; Yang, H. Solvothermal synthesis of InP quantum dots and their enhanced luminescent efficiency by post-synthetic treatments. *J. Colloid Interface Sci.* **2011**, *355*, 35−41.
(47) Qian, Y. Solvothermal Synthesis of Nanocrystalline III−V Semiconductors. *Adv. Mater.* **1999**, *11*, 1101−1102.
(48) Hens, Z.; Capek, R. K. Size tuning at full yield in the synthesis of colloidal semiconductor nanocrystals, reaction simulations and experimental verification. *Coord. Chem. Rev.* **2014**, *263*, 217−228.

DOI: 10.1021/acs.chemmater.5b05044
Chem. Mater. 2016, 28, 2491−2506

(49) Hendricks, M. P.; Campos, M. P.; Cleveland, G. T.; Jen-La Plante, I.; Owen, J. S. A tunable library of substituted thiourea precursors to metal sulfide nanocrystals. *Science* **2015**, *348*, 1226−1230.
(50) Rempel, J. Y.; Bawendi, M. G.; Jensen, K. F. Insights into the Kinetics of Semiconductor Nanocrystal Nucleation and Growth. *J. Am. Chem. Soc.* **2009**, *131*, 4479−4489.
(51) Liu, H. T.; Owen, J. S.; Alivisatos, A. P. Mechanistic study of precursor evolution in colloidal group II-VI semiconductor nanocrystal synthesis. *J. Am. Chem. Soc.* **2007**, *129*, 305−312.
(52) Franke, D.; Harris, D. K.; Xie, L.; Jensen, K. F.; Bawendi, M. G. The Unexpected Influence of Precursor Conversion Rate for III−V Quantum Dots. *Angew. Chem.* **2015**, *127*, 14507−14511.
(53) Harris, D. K.; Bawendi, M. G. Improved Precursor Chemistry for the Synthesis of III-V Quantum Dots. *J. Am. Chem. Soc.* **2012**, *134*, 20211−20213.
(54) Gary, D. C.; Glassy, B. A.; Cossairt, B. M. Investigation of Indium Phosphide Quantum Dot Nucleation and Growth Utilizing Triarylsilylphosphine Precursors. *Chem. Mater.* **2014**, *26*, 1734−1744.
(55) Reiss, H. The Growth of Uniform Colloidal Dispersions. *J. Chem. Phys.* **1951**, *19*, 482−487.
(56) Talapin, D. V.; Rogach, A. L.; Haase, M.; Weller, H. Evolution of an Ensemble of Nanoparticles in a Colloidal Solution: Theoretical Study. *J. Phys. Chem. B* **2001**, *105*, 12278−12285.
(57) Marqusee, J. A.; Ross, J. Theory of Ostwald ripening: Competitive growth and its dependence on volume fraction. *J. Chem. Phys.* **1984**, *80*, 536−543.
(58) Peng, X. G.; Wickham, J.; Alivisatos, A. P. Kinetics of II-VI and III-V colloidal semiconductor nanocrystal growth: "Focusing" of size distributions. *J. Am. Chem. Soc.* **1998**, *120*, 5343−5344.
(59) Clark, M. D.; Kumar, S. K.; Owen, J. S.; Chan, E. M. Focusing Nanocrystal Size Distributions via Production Control. *Nano Lett.* **2011**, *11*, 1976−1980.
(60) Allen, P. M.; Walker, B. J.; Bawendi, M. G. Mechanistic Insights into the Formation of InP Quantum Dots. *Angew. Chem., Int. Ed.* **2010**, *49*, 760−762.
(61) Thuy, U. T. D.; Huyen, T. T. T.; Liem, N. Q.; Reiss, P. Low temperature synthesis of InP nanocrystals. *Mater. Chem. Phys.* **2008**, *112*, 1120−1123.
(62) Green, M.; O'Brien, P. A novel metalorganic route for the direct and rapid synthesis of monodispersed quantum dots of indium phosphide. *Chem. Commun.* **1998**, 2459−2460.
(63) Jun, K.-W.; Khanna, P. K.; Hong, K.-B.; Baeg, J.-O.; Suh, Y.-D. Synthesis of InP nanocrystals from indium chloride and sodium phosphide by solution route. *Mater. Chem. Phys.* **2006**, *96*, 494−497.
(64) Liu, Z.; Kumbhar, A.; Xu, D.; Zhang, J.; Sun, Z.; Fang, J. Coreduction Colloidal Synthesis of III−V Nanocrystals: The Case of InP. *Angew. Chem.* **2008**, *120*, 3596−3598.
(65) Li, L.; Protière, M.; Reiss, P. Economic Synthesis of High Quality InP Nanocrystals Using Calcium Phosphide as the Phosphorus Precursor. *Chem. Mater.* **2008**, *20*, 2621−2623.
(66) Joung, S.; Yoon, S.; Han, C.-S.; Kim, Y.; Jeong, S. Facile synthesis of uniform large-sized InP nanocrystal quantum dots using tris(tert-butyldimethylsilyl)phosphine. *Nanoscale Res. Lett.* **2012**, *7*, 93.
(67) Amberger, E.; Salazar G, R. W. Mixed organometallic compounds of group V I. Synthesis of tris(trimethyl-group-IV)stibines. *J. Organomet. Chem.* **1967**, *8*, 111−114.
(68) Gary, D. C.; Terban, M. W.; Billinge, S. J. L.; Cossairt, B. M. Two-Step Nucleation and Growth of InP Quantum Dots via Magic-Sized Cluster Intermediates. *Chem. Mater.* **2015**, *27*, 1432−1441.
(69) Dukes, A. D.; McBride, J. R.; Rosenthal, S. J. Synthesis of Magic-Sized CdSe and CdTe Nanocrystals with Diisooctylphosphinic Acid. *Chem. Mater.* **2010**, *22*, 6402−6408.
(70) Cossairt, B. M.; Owen, J. S. CdSe Clusters: At the Interface of Small Molecules and Quantum Dots. *Chem. Mater.* **2011**, *23*, 3114−3119.
(71) Harrell, S. M.; McBride, J. R.; Rosenthal, S. J. Synthesis of Ultrasmall and Magic-Sized CdSe Nanocrystals. *Chem. Mater.* **2013**, *25*, 1199−1210.
(72) Li, M.; Ouyang, J.; Ratcliffe, C. I.; Pietri, L.; Wu, X.; Leek, D. M.; Moudrakovski, I.; Lin, Q.; Yang, B.; Yu, K. CdS Magic-Sized Nanocrystals Exhibiting Bright Band Gap Photoemission via Thermodynamically Driven Formation. *ACS Nano* **2009**, *3*, 3832−3838.
(73) Evans, C. M.; Guo, L.; Peterson, J. J.; Maccagnano-Zacher, S.; Krauss, T. D. Ultrabright PbSe Magic-sized Clusters. *Nano Lett.* **2008**, *8*, 2896−2899.
(74) Xie, R.; Peng, X. Synthetic Scheme for High-Quality InAs Nanocrystals Based on Self-Focusing and One-Pot Synthesis of InAs-Based Core−Shell Nanocrystals. *Angew. Chem., Int. Ed.* **2008**, *47*, 7677−7680.
(75) Xie, R.; Li, Z.; Peng, X. Nucleation Kinetics vs Chemical Kinetics in the Initial Formation of Semiconductor Nanocrystals. *J. Am. Chem. Soc.* **2009**, *131*, 15457−15466.
(76) Gary, D. C.; Flowers, S. E.; Kaminsky, W.; Petrone, A.; Li, X.; Cossairt, B. M. Single-Crystal and Electronic Structure of a 1.3 nm Indium Phosphide Nanocluster. *J. Am. Chem. Soc.* **2016**, *138*, 1510.
(77) Song, W.-S.; Lee, H.-S.; Lee, J.; Jang, D.; Choi, Y.; Choi, M.; Yang, H. Amine-derived synthetic approach to color-tunable InP/ZnS quantum dots with high fluorescent qualities. *J. Nanopart. Res.* **2013**, *15*, 1750.
(78) Byun, H.-J.; Song, W.-S.; Yang, H. Facile consecutive solvothermal growth of highly fluorescent InP/ZnS core/shell quantum dots using a safer phosphorus source. *Nanotechnology* **2011**, *22*, 235605.
(79) Tessier, M. D.; Dupont, D.; De Nolf, K.; De Roo, J.; Hens, Z. Economic and Size-Tunable Synthesis of InP/ZnE (E = S, Se) Colloidal Quantum Dots. *Chem. Mater.* **2015**, *27*, 4893−4898.
(80) Kim, K.; Yoo, D.; Choi, H.; Tamang, S.; Ko, J.-H.; Kim, S.; Kim, Y.-H.; Jeong, S. Halide−Amine Co-Passivated Indium Phosphide Colloidal Quantum Dots in Tetrahedral Shape. *Angew. Chem., Int. Ed.* **2016**, *55*, 3714−3718.
(81) Cros-Gagneux, A.; Delpech, F.; Nayral, C.; Cornejo, A.; Coppel, Y.; Chaudret, B. Surface Chemistry of InP Quantum Dots: A Comprehensive Study. *J. Am. Chem. Soc.* **2010**, *132*, 18147−18157.
(82) Virieux, H.; Le Troedec, M.; Cros-Gagneux, A.; Ojo, W.-S.; Delpech, F.; Nayral, C.; Martinez, H.; Chaudret, B. InP/ZnS Nanocrystals: Coupling NMR and XPS for Fine Surface and Interface Description. *J. Am. Chem. Soc.* **2012**, *134*, 19701−19708.
(83) Xie, L.; Harris, D. K.; Bawendi, M. G.; Jensen, K. F. Effect of Trace Water on the Growth of Indium Phosphide Quantum Dots. *Chem. Mater.* **2015**, *27*, 5058−5063.
(84) Gary, D. C.; Cossairt, B. M. Role of Acid in Precursor Conversion During InP Quantum Dot Synthesis. *Chem. Mater.* **2013**, *25*, 2463−2469.
(85) Narayanaswamy, A.; Xu, H.; Pradhan, N.; Kim, M.; Peng, X. Formation of Nearly Monodisperse In2O3 Nanodots and Oriented-Attached Nanoflowers: Hydrolysis and Alcoholysis vs Pyrolysis. *J. Am. Chem. Soc.* **2006**, *128*, 10310−10319.
(86) Franke, D.; Harris, D. K.; Xie, L.; Jensen, K. F.; Bawendi, M. G. The Unexpected Influence of Precursor Conversion Rate for III−V Quantum Dots. *Angew. Chem., Int. Ed.* **2015**, *54*, 14299−14303.
(87) Xie, R.; Battaglia, D.; Peng, X. Colloidal InP Nanocrystals as Efficient Emitters Covering Blue to Near-Infrared. *J. Am. Chem. Soc.* **2007**, *129*, 15432−15433.
(88) Protiere, M.; Reiss, P. Amine-induced growth of an In2O3 shell on colloidal InP nanocrystals. *Chem. Commun.* **2007**, 2417−2419.
(89) Gooßen, L. J.; Ohlmann, D. M.; Lange, P. P. The Thermal Amidation of Carboxylic Acids Revisited. *Synthesis* **2009**, *2009*, 160−164.
(90) Anderson, N. C.; Hendricks, M. P.; Choi, J. J.; Owen, J. S. Ligand Exchange and the Stoichiometry of Metal Chalcogenide Nanocrystals: Spectroscopic Observation of Facile Metal-Carboxylate Displacement and Binding. *J. Am. Chem. Soc.* **2013**, *135*, 18536−18548.
(91) Thuy, U. T. D.; Reiss, P.; Liem, N. Q. Luminescence properties of In(Zn)P alloy core/ZnS shell quantum dots. *Appl. Phys. Lett.* **2010**, *97*, 193104.

DOI: 10.1021/acs.chemmater.5b05044
Chem. Mater. 2016, 28, 2491−2506

(92) Ryu, E.; Kim, S.; Jang, E.; Jun, S.; Jang, H.; Kim, B.; Kim, S.-W. Step-Wise Synthesis of InP/ZnS Core-Shell Quantum Dots and the Role of Zinc Acetate. *Chem. Mater.* **2009**, *21*, 573−575.
(93) Beberwyck, B. J.; Surendranath, Y.; Alivisatos, A. P. Cation Exchange: A Versatile Tool for Nanomaterials Synthesis. *J. Phys. Chem. C* **2013**, *117*, 19759−19770.
(94) Beberwyck, B. J.; Alivisatos, A. P. Ion Exchange Synthesis of III-V Nanocrystals. *J. Am. Chem. Soc.* **2012**, *134*, 19977−19980.
(95) De Trizio, L.; Gaspari, R.; Bertoni, G.; Kriegel, I.; Moretti, L.; Scotognella, F.; Maserati, L.; Zhang, Y.; Messina, G. C.; Prato, M.; Marras, S.; Cavalli, A.; Manna, L. Cu3-xP Nanocrystals as a Material Platform for Near-Infrared Plasmonics and Cation Exchange Reactions. *Chem. Mater.* **2015**, *27*, 1120−1128.
(96) Reiss, P.; Protiere, M.; Li, L. Core/Shell Semiconductor Nanocrystals. *Small* **2009**, *5*, 154−168.
(97) Haubold, S.; Haase, M.; Kornowski, A.; Weller, H. Strongly Luminescent InP/ZnS Core−Shell Nanoparticles. *ChemPhysChem* **2001**, *2*, 331−334.
(98) Kim, M. R.; Chung, J. H.; Lee, M.; Lee, S.; Jang, D.-J. Fabrication, spectroscopy, and dynamics of highly luminescent core@shell InP@ZnSe quantum dots. *J. Colloid Interface Sci.* **2010**, *350*, 5−9.
(99) Mićić, O. I.; Smith, B. B.; Nozik, A. J. Core/shell Quantum Dots of Lattice-Matched ZnCdSe2 Shells on InP Cores: Experiment and Theory. *J. Phys. Chem. B* **2000**, *104*, 12149−12156.
(100) Lim, J.; Bae, W. K.; Lee, D.; Nam, M. K.; Jung, J.; Lee, C.; Char, K.; Lee, S. InP@ZnSeS, Core@Composition Gradient Shell Quantum Dots with Enhanced Stability. *Chem. Mater.* **2011**, *23*, 4459−4463.
(101) Kim, S.; Fisher, B.; Eisler, H.-J.; Bawendi, M. Type-II Quantum Dots: CdTe/CdSe(Core/Shell) and CdSe/ZnTe(Core/Shell) Heterostructures. *J. Am. Chem. Soc.* **2003**, *125*, 11466−11467.
(102) Park, J.; Kim, S.; Kim, S.; Yu, S. T.; Lee, B.; Kim, S.-W. Fabrication of highly luminescent InP/Cd and InP/CdS quantum dots. *J. Lumin.* **2010**, *130*, 1825−1828.
(103) Talapin, D. V.; Rogach, A. L.; Kornowski, A.; Haase, M.; Weller, H. Highly Luminescent Monodisperse CdSe and CdSe/ZnS Nanocrystals Synthesized in a Hexadecylamine-Trioctylphosphine Oxide-Trioctylphospine Mixture. *Nano Lett.* **2001**, *1*, 207−211.
(104) Lim, J.; Park, M.; Bae, W. K.; Lee, D.; Lee, S.; Lee, C.; Char, K. Highly Efficient Cadmium-Free Quantum Dot Light-Emitting Diodes Enabled by the Direct Formation of Excitons within InP@ZnSeS Quantum Dots. *ACS Nano* **2013**, *7*, 9019−9026.
(105) Dabbousi, B. O.; Rodriguez-Viejo, J.; Mikulec, F. V.; Heine, J. R.; Mattoussi, H.; Ober, R.; Jensen, K. F.; Bawendi, M. G. (CdSe)ZnS Core/shell Quantum Dots: Synthesis and Characterization of a Size Series of Highly Luminescent Nanocrystallites. *J. Phys. Chem. B* **1997**, *101*, 9463−9475.
(106) Huang, K.; Demadrille, R.; Silly, M. G.; Sirotti, F.; Reiss, P.; Renault, O. Internal Structure of InP/ZnS Nanocrystals Unraveled by High-Resolution Soft X-ray Photoelectron Spectroscopy. *ACS Nano* **2010**, *4*, 4799−4805.
(107) Protiere, M.; Reiss, P. Facile synthesis of monodisperse ZnS capped CdS nanocrystals exhibiting efficient blue emission. *Nanoscale Res. Lett.* **2006**, *1*, 62−67.
(108) Xie, R. G.; Kolb, U.; Li, J. X.; Basche, T.; Mews, A. Synthesis and characterization of highly luminescent CdSe-Core CdS/Zn0.5Cd0.5S/ZnS multishell nanocrystals. *J. Am. Chem. Soc.* **2005**, *127*, 7480−7488.
(109) Xi, L.; Cho, D.-Y.; Duchamp, M.; Boothroyd, C. B.; Lek, J. Y.; Besmehn, A.; Waser, R.; Lam, Y. M.; Kardynal, B. Understanding the Role of Single Molecular ZnS Precursors in the Synthesis of In(Zn)P/ZnS Nanocrystals. *ACS Appl. Mater. Interfaces* **2014**, *6*, 18233−18242.
(110) Kahen, K.; Holland, M.; Kuttiatoor, S. US2013-0092886, 2013
(111) Erwin, S. C.; Zu, L.; Haftel, M. I.; Efros, A. L.; Kennedy, T. A.; Norris, D. J. Doping semiconductor nanocrystals. *Nature* **2005**, *436*, 91−94.
(112) Sahu, A.; Kang, M. S.; Kompch, A.; Notthoff, C.; Wills, A. W.; Deng, D.; Winterer, M.; Frisbie, C. D.; Norris, D. J. Electronic Impurity Doping in CdSe Nanocrystals. *Nano Lett.* **2012**, *12*, 2587−2594.
(113) Norris, D. J.; Efros, A. L.; Erwin, S. C. Doped Nanocrystals. *Science* **2008**, *319*, 1776−1779.
(114) Mocatta, D.; Cohen, G.; Schattner, J.; Millo, O.; Rabani, E.; Banin, U. Heavily Doped Semiconductor Nanocrystal Quantum Dots. *Science* **2011**, *332*, 77−81.
(115) Xie, R.; Peng, X. Synthesis of Cu-Doped InP Nanocrystals (d-dots) with ZnSe Diffusion Barrier as Efficient and Color-Tunable NIR Emitters. *J. Am. Chem. Soc.* **2009**, *131*, 10645−10651.
(116) Knowles, K. E.; Nelson, H. D.; Kilburn, T. B.; Gamelin, D. R. Singlet−Triplet Splittings in the Luminescent Excited States of Colloidal Cu+:CdSe, Cu+:InP, and CuInS2 Nanocrystals: Charge-Transfer Configurations and Self-Trapped Excitons. *J. Am. Chem. Soc.* **2015**, *137*, 13138−13147.
(117) Zhang, Z.; Liu, D.; Li, D.; Huang, K.; Zhang, Y.; Shi, Z.; Xie, R.; Han, M.-Y.; Wang, Y.; Yang, W. Dual Emissive Cu:InP/ZnS/InP/ZnS Nanocrystals: Single-Source "Greener" Emitters with Flexibly Tunable Emission from Visible to Near-Infrared and Their Application in White Light-Emitting Diodes. *Chem. Mater.* **2015**, *27*, 1405−1411.
(118) Li, J. J.; Wang, Y. A.; Guo, W. Z.; Keay, J. C.; Mishima, T. D.; Johnson, M. B.; Peng, X. G. Large-scale synthesis of nearly monodisperse CdSe/CdS core/shell nanocrystals using air-stable reagents via successive ion layer adsorption and reaction. *J. Am. Chem. Soc.* **2003**, *125*, 12567−12575.
(119) Thuy, U. T. D.; Maurice, A.; Liem, N. Q.; Reiss, P. Europium doped In(Zn)P/ZnS colloidal quantum dots. *Dalton Trans.* **2013**, *42*, 12606−12610.
(120) Phillips, J. C. *Bonds and bands in semiconductors*; Academic Press: New York, 1973.
(121) Guzelian, A. A.; Banin, U.; Kadavanich, A. V.; Peng, X.; Alivisatos, A. P. Colloidal chemical synthesis and characterization of InAs nanocrystal quantum dots. *Appl. Phys. Lett.* **1996**, *69*, 1432−1434.
(122) Evans, C. M.; Castro, S. L.; Worman, J. J.; Raffaelle, R. P. Synthesis and Use of Tris(trimethylsilyl)antimony for the Preparation of InSb Quantum Dots. *Chem. Mater.* **2008**, *20*, 5727−5730.
(123) Zhang, J.; Zhang, D. Synthesis and growth kinetics of high quality InAs nanocrystals using in situ generated AsH3 as the arsenic source. *CrystEngComm* **2010**, *12*, 591−594.
(124) Maurice, A.; Haro, M. L.; Hyot, B.; Reiss, P. Synthesis of Colloidal Indium Antimonide Nanocrystals Using Stibine. *Particle Particle Systems Characterization* **2013**, *30*, 828−831.
(125) Liu, W.; Chang, A. Y.; Schaller, R. D.; Talapin, D. V. Colloidal InSb Nanocrystals. *J. Am. Chem. Soc.* **2012**, *134*, 20258−20261.
(126) Yarema, M.; Kovalenko, M. V. Colloidal Synthesis of InSb Nanocrystals with Controlled Polymorphism Using Indium and Antimony Amides. *Chem. Mater.* **2013**, *25*, 1788−1792.
(127) Tamang, S.; Kim, K.; Choi, H.; Kim, Y.; Jeong, S. Synthesis of colloidal InSb nanocrystals via in situ activation of InCl3. *Dalton Trans.* **2015**, *44*, 16923−16928.
(128) Xie, L.; Zhao, Q.; Jensen, K. F.; Kulik, H. J. Direct Observation of Early-Stage Quantum Dot Growth Mechanisms with High-Temperature Ab Initio Molecular Dynamics. *J. Phys. Chem. C* **2016**, *120*, 2472−2483.
(129) Baumgartner, J.; Dey, A.; Bomans, P. H. H.; Le Coadou, C.; Fratzl, P.; Sommerdijk, N. A. J. M.; Faivre, D. Nucleation and growth of magnetite from solution. *Nat. Mater.* **2013**, *12*, 310−314.
(130) Zhao, Q.; Xie, L.; Kulik, H. J. Discovering Amorphous Indium Phosphide Nanostructures with High-Temperature ab Initio Molecular Dynamics. *J. Phys. Chem. C* **2015**, *119*, 23238−23249.

DOI: 10.1021/acs.chemmater.5b05044
Chem. Mater. 2016, 28, 2491−2506